AN INVESTIGATION OF MAGNETIC FLOAT POLISHING TECHNIQUES INCLUDING CONVENTIONAL, ECCENTRIC SHAFT, AND ULTRASONIC ASSISTED POLISHING.

By

BRIAN DOUGLAS PERRY

Bachelor of Science

Oklahoma State University

Stillwater, Oklahoma

1995

Submitted to the Faculty of the
Graduate College of the
Oklahoma State University
in partial fullfillment of
the requirements for
the degree of
MASTER OF SCIENCE
December, 1997

AN INVESTIGATION OF MAGNETIC FLOAT POLISHING TECHNIQUES INCLUDING CONVENTIONAL, ECCENTRIC SHAFT, AND ULTRASONIC ASSISTED POLISHING.

Thesis Approved:

Thesis Adviser

Don A. Lucca

Ronald L. Dougherty

Thomas C. Collins

Dean of the Graduate College

SUMMARY

Ceramic materials offer material properties that make them ideal candidates for use in ball bearing applications. These material properties include high compression strength, very high hardness, high wear resistance, and high temperature capabilities. By incorporating ceramic balls with steel races to create a hybrid ball bearing, a superior product is created that is capable of higher rpm's, higher temperature capabilities, lower lubrication requirements, and longer service life.

Unfortunately, the same properties that make ceramics ideal for bearing use, also make them very difficult to manufacture to the high tolerances required for bearing use. The current industry practice is to use a V-groove lapping process with diamond slurry. This process uses very high forces, low rotation speeds, and very long polishing times. The high forces and hard diamond abrasives combine to create a lot of surface damage to the ceramic elements, that require long periods of time with small abrasives to repair.

Magnetic Float Polishing (MFP) is a technique that has been developed that processes ceramic balls with little or no surface damage. This MFP process, which incorporates the use of magnetic fluid levitation, uses higher rpm's lower loads, and softer abrasives. The result is a ball that is finished in a fraction of the time needed with V-groove lapping. One drawback is that,

currently, the results of the MFP process cannot quite match the results of the V-groove lapping, with respect to sphericity.

The MFP process came about as a result of the evolution of many different techniques incorporating magnetic fluid in a machining process. The investigation documented here follows this spirit of evaluation and experimentation in order to improve upon the current state of the art.

Three different aspects of MFP are considered in this investigation. First is the conventional method of MFP adapted to a new size of balls not previously considered. In the design of the new chamber, material choice and construction techniques are chosen in order to increase the dimensional accuracy of the chamber. This attention to dimensional tolerances is implemented in the hopes that it will improve the sphericity results of the balls.

The second aspect of this investigation looks into the use of an eccentric, or offset, polishing shaft. The use of an eccentric shaft has been reported to achieve better sphericity results and higher MRR's. An eccentric shaft chamber is built and tested in order to evaluate the effectiveness of the eccentric shaft in producing better finished products.

The third aspect covered here is the combination, or superposition, of the MFP process with the ultrasonic machining process. Ultrasonic machining is a process that is similar to the MFP process, in that, they both rely on an abrasive slurry to remove material. It is hoped that by combining the two technologies, a superior final product can be achieved. Choice of transducer and placement of the transducer are two topics that must be considered when combining these two

processes. In addition, a power supply must be chosen and incorporated to route the ultrasonic signal to the transducer.

These three topics are examined and evaluated in this investigation. Items used to evaluate the effectiveness of a given process are the sphericity and the surface finish of the balls produced, and the MRR achieved during the process. Improved sphericity and surface finish will result in a higher bearing quality (lower ANSI grade number). Increased MRR will help to reduce the time required to process the balls from start to finish, which will ultimately result in a lower cost.

ACKNOWLEDGMENTS

First and foremost, I would like to express my gratitude towards Dr. R. Komanduri for his guidance and inspiration. Special thanks are also due to Drs. D.A. Lucca, and R.L. Dougherty for taking the time to serve on my committee.

This project was sponsored by grants from the National Science Foundation (CMS-9414610, DMI-9402895, DAAH04-96-1-0323). Initial funding for early work on this project was provided by ARPA (F33615-92-5933). Additional funding was supplied by the CATTS project. Thanks are due towards Drs. J. Larsen Basse, B.M. Kramer, Ming Leu, and J. Lee of the NSF, and Dr. K.R. Mecklenburg of Wright Patterson Air Force Base, and Dr. W. Coblenz of DARPA for expressing interest in these research activities.

I would also like to thank Dr. Makaram Raghunandan, Dr. Ali Noori-Khajavi, Mr. Baghavatula, Dr. Noritsugu Umehara, and Dr. Bo Zhang, for their valuable assistance and support with this research.

In addition, I would like to extend my gratitude towards my colleagues, Ming Jiang, Murat Cetin, Vinoo Thomas, Johnnie Hixson, Robert Stewart, Dave Stokes, Naga Chandrasekaran, K. Mallika, and Rajesh Iyer for their valuable help and friendship throughout my stay at OSU.

On a personal note, I would like to extend a special thanks to my parents, Bob and Mary Perry for their continuous encouragement and support, both personally and financially. I could not have done it without you. Thanks also to the rest of my family and friends for your support in my endeavors.

TABLE OF CONTENTS

LIST OF FIGURES

Figure Page

LIST OF TABLES

CHAPTER 1

INTRODUCTION

Advanced ceramic materials offer many characteristics that are desirable for use in many engineering applications. Among these are high strength, high hardness, and good wear resistance. Unfortunately these same characteristics also make the ceramic materials difficult to manufacture into usable shapes. One application in particular where ceramic materials excel is in the hybrid bearing market. Hybrid bearings consist of steel races and cages with ceramic balls. With this configuration, the bearings can perform at much higher speeds and higher loads for longer periods of time with little or no lubrication.

This application of ceramic materials requires very precise geometry and good surface finish. The conventional industrial method for manufacturing these balls is a diamond lapping process. This process uses two plates with V-grooves that hold the balls. Compression force is applied and the plates are rotated with a diamond abrasive slurry added to the work area. Since the diamond abrasive is harder than the ceramic, material is removed from the ceramic balls by brittle fracture. Progressively smaller grit sizes are used to improve the sphericity (roundness) and surface finish of the balls. When

removing material by brittle fracture, you also introduce surface defects into the work material. Surface defects and near-surface defects are of great importance, since the balls are loaded in compression, and any catastrophic failure will invariably initiate from the surface. This is one area where the current industrial practice falls short. Another drawback to this method is the great amount of time required to finish a set of balls completely.

Magnetic float polishing (MFP) is a technique that was developed as an alternate method for finishing ceramic balls. This method shows much higher material removal rates, anywhere from 50 to 100 times higher, so a batch of balls can be finished in much shorter amount of time. In addition abrasive particles that are actually softer than the work material can be used to remove material by a chemo-mechanical action. Since there is no brittle fracture involved in chemo-mechanical finishing, a 'defect free' surface can be achieved. The purpose of this investigation is to evaluate the MFP process, and a few variations on the process in order to achieve better results faster.

1.1 Background

The MFP process is the result of the evolution of many techniques involving magnetic fluid in many different ways to improve upon, and in some cases create new, methods of machining. These different processes can all be

categorized as Magnetic Field Assisted Machining. This can then be divided into two sub categories: Magnetic Float Polishing, and Magnetic Abrasive Finishing. The main difference between the two is that MFP uses a magnetic fluid, where the MAF process uses magnetic abrasive particles.

1.1.1 Magnetic Abrasive Finishing

The MAF process uses abrasive particles mixed in with iron particles to finish a wide variety of surfaces. Typical surfaces finished with this technique are interior and exterior cylindrical surface, and cylinder ends. The iron particles are drawn to the magnets and carry the abrasive particles along, forming a sort of brush. This brush is then used to polish the desired surface. Figure 1.1 below shows a typical setup where the abrasive brush is used to polish the exterior surface of a cylinder. This method can be used to manufacture rollers for use in roller bearings.

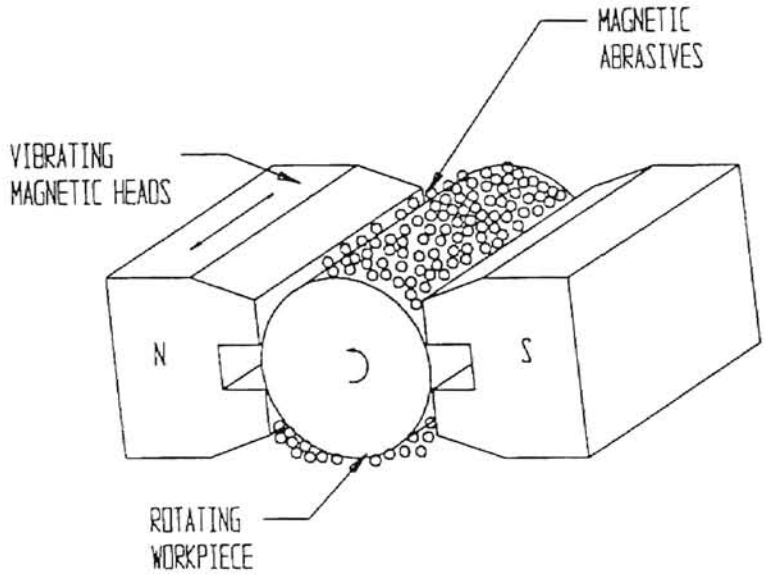

Figure 1.1 - Typical Magnetic Abrasive Finishing Setup

This method has the advantages of being able to get abrasive particles into difficult areas, and to provide gentle polishing action to get good surface finish on these hard to reach areas.

1.1.2 Magnetic Float Polishing

The process of MFP began as a method for finishing the end of cylidrical surfaces. Initially no float was used, magnetic fluid mixed with abrasive particles was poured directly over a bank of permanent magnets. The fluid was drawn to the magnets, creating a sort of fluid 'pad'. The non-magnetic abrasive particles are forced towards the top of this pad, such that when a flat surface is introduced into the system, the abrasive particles are pushed into the surface. The flat surface is then rotated through the fluid, and the polishing action occurs. Figure 1.2.a below shows the process called Hydro-magnetic Grinding (Umehara and Kato, 1987).

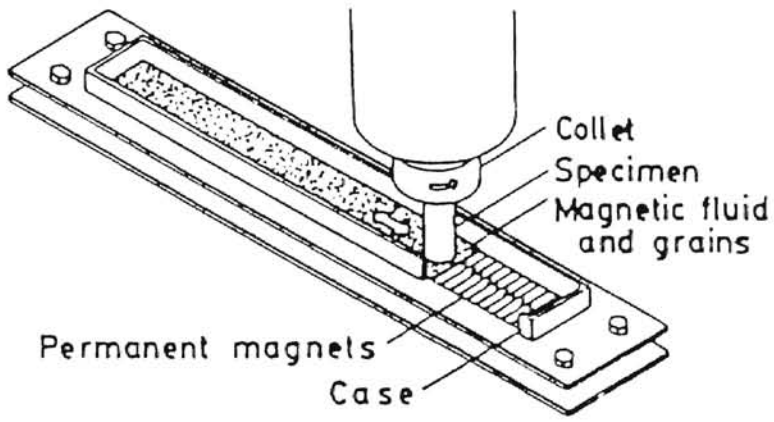

Figure 1.2 - Hydro-magnetic Grinding Apparatus (Umehara and Kato, 1987)

It was noted by this group of researchers that increased grinding forces would be achieved by introducing a non-magnetic float. Increased grinding forces results in higher material removal rates, which results in shorter finishing times. Figure 1.3 shows a) the difference between the two processes, and b) the difference in force achieved between the two.

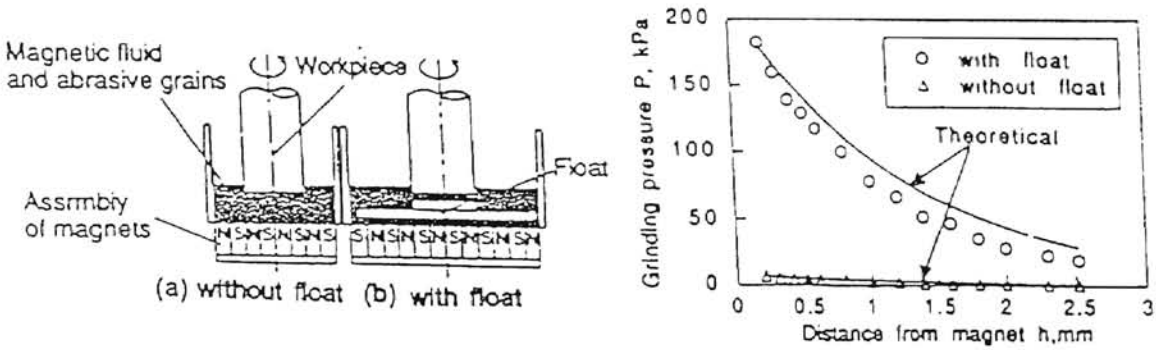

Figure 1.3 - a) Magnetic fluid grinding schematic with and without float
b) Difference in forces achieved with and without float (Umehara, 1994)

From this point the setup is modified in order to accommodate the ball geometry. Instead of the rotating shaft being the workpiece, it becomes the tool, with the balls being placed between the shaft and the float. This is the technique that is known as Magnetic Float Polishing. This method is used to achieve very good results in a fraction of the time necessary with conventional diamond lapping. The figure below shows a schematic of the apparatus used in this investigation. This technique uses a variety of abrasive particles, and can be used from 1,000 - 20,000 rpm, so it is a very versatile process. The chamber is relatively easy to manufacture, and can be adapted to any milling machine.

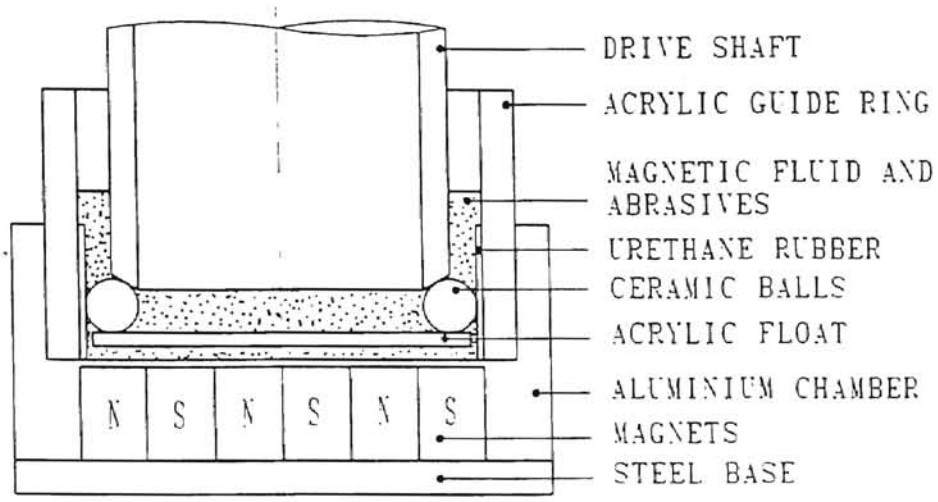

Figure 1.4 - Magnetic Float Polishing Apparatus

1.2 Silicon Nitride Work Material

The material used for this investigation is hot isostatically pressed (HIP) silicon nitride. This material is known for its very high hardness, high resistance to wear and high toughness (compared to other ceramic materials), and low density. The HIPing process begins with a powder form of the material. This powder material is then heated to about 1700 °C, in a nitrogen atmosphere, at high pressures of about 300 MPa. When in this state it is compacted into the desired shape. Compared to other manufacturing techniques, HIPing provides a nearly fully theoretically dense product. By being closer to theoretical density, the mechanical properties are enhanced. Table 1.1 below gives various properties of silicon nitride.

1.3 Abrasives Used

During these tests various abrasive types are used for different stages of finishing. Harder materials and larger grain sizes are used in the initial stages to remove large amounts of material, and to bring the balls towards the desired sphericity. Towards the end stage, softer and smaller size abrasive particles are used in order to get final sphericity and final surface finish properties. In some cases, in particular chromium oxide, the abrasive is actually softer than the work material, and a chemo-mechanical action is observed to remove material. Particle sizes of the abrasives range from ~40 μm (500 grain) to <1 μm (8000 grain). All of the abrasives used are ceramic powders, and are relatively cheap when compared to the cost of diamond abrasives used in conventional lapping. This is a major cost saving feature of the MFP process. The following table lists the various abrasives used and their respective hardness values. Note that some are equal to or less than the hardness value of silicon nitride, which results in little, if any, surface defects introduced by the abrasive.

1.4 Magnetic Fluid

A magnetic fluid is a carrier fluid that has sub-domain particles suspended within it that respond to magnetic fields. These particles are on the order of 100 angstroms, and are coated with a stabilizing dispersing agent to prevent falling out of the carrier liquid. The fluid itself is not capable of sustaining a magnetic charge, since the particles align randomly within the fluid. Once a magnetic field is introduced to the fluid, the particles are attracted to the magnetic field lines

Table 1.1 - Properties of Silicon Nitride

Crystal Structure	
α phase - hexagonal	a = 0.775 - 0.777 nm c = 0.516 - 0.569 nm
β phase - hexagonal	a = 0.759 - 0.761 nm c = 0.271 - 0.292 nm
Decomposition Temp	1900 °C
Theoretical Density	
α phase	3.16 - 3.19 g/cm^3
β phase	3.19 - 3.20 g/cm^3
Coefficient of Thermal Expansion	2.9 - 3.6 x 10^6 / °C
Thermal Conductivity	15 - 50 W/m/K
Thermal Diffusivity	0.08 - 0.29 cm^2/s
Specific Heat	700 J/kg/°C
Hardness (Vickers)	1600 - 2200 Mpa
Young's Modulus	300 - 330 Gpa
Fracture Toughness	3.4 - 8.2 MN m$^{-3/2}$

When this occurs the fluid appears to 'gel' around the field lines, while still retaining its viscous properties. This behavior causes any foreign objects within

the fluid to be expelled away from the magnetic field. This is known as magnetic fluid levitation, and is the principle behind MFP.

Table 1.2 - Properties of Abrasives Used

Material	Hardness (Vickers)	Density (g/cm^3)	Melting Point (°C)
Diamond (C)	>8000	3.5	>3500
Boron Carbide (B_4C)	3400	2.5	2450
Silicon Carbide (SiC)	2500	3.2	2400
Aluminum Oxide (Al_2O_3)	2100	4.0	2040
Chromium Oxide (Cr_2O_3)	2000 - 2200	5.2	2265

CHAPTER 2

LITERATURE REVIEW

Magnetic float polishing is a technique that is the result of an evolution of many different methods of polishing using magnetic fluid or magnetic abrasives. Among the first known use of magnetic assisted finishing techniques is Coats, who in 1940 used magnetic abrasives to finish the interior surface of barrels. This led to the use of MAF to finish a variety of shapes. The idea of using magnetic forces to assist in polishing caught on and many different uses for magnetic fluid were found.

2.1 Development of MFP

Imanka (1981) was an early researcher of magnetic fluid, and its applications to polishing. Magnetic fluid was enclosed in a membrane, which was inside a polishing chamber. The chamber was placed over a magnetic base, and an abrasive slurry was placed in the chamber. Pieces to be polished were placed in the chamber from above and lowered against the magnetic 'pad'. This created the compressive force necessary for polishing. Figure 2.1 gives a schematic of this early use of magnetic fluid for polishing.

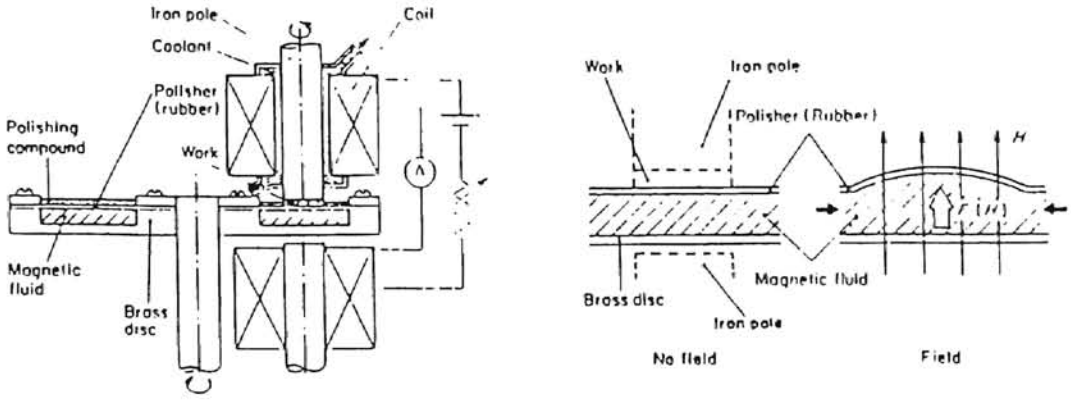

Figure 2.1 - Polishing Setup Used by Imanka (1981)

Tani and Kawata (1984) took this idea one step further. By eliminating the membrane, and mixing the abrasive particles directly into the magnetic fluid, higher removal rates can be seen. The particles tend to extract out of the fluid, due to the fact that they are non-magnetic, and accumulate at the surface of the fluid pad. This creates a direct compressive force on the abrasive particles, and when a workpiece is rotated through the fluid, higher material removal rates occur.

Umehara and Kato (1987) incorporated magnetic fluid into the polishing of borosilicate glass. Polishing of the glass was done by rotating a stylus or tool that was columnar in shape and was suspended from the top. A magnet was placed at the lower end of the stylus, and a quantity of magnetic fluid with abrasive mixed in was added. Again the magnetic forces tend to extract the abrasive particles and gather them at the surface of the magnetic fluid pad. The stylus is then rotated to get the polishing action. This type of magnetic fluid

polishing is useful for grinding of glass for use with lenses and mirrors. Figure 2.2 shows a diagram of the apparatus used for polishing of glass.

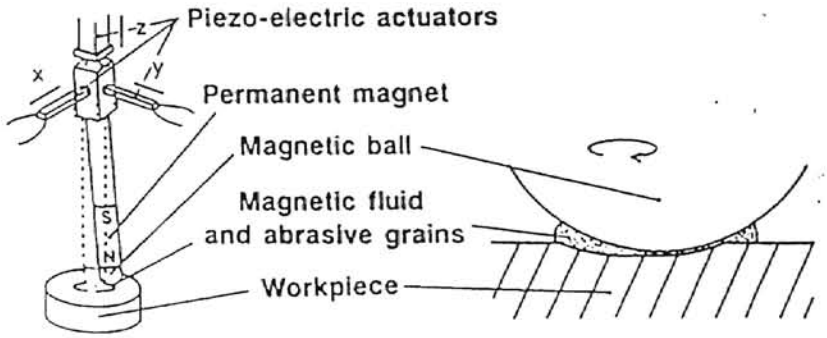

Figure 2.2 - Polishing of Borosilicate Glass with Magnetic Fluid (Umehara and Kato, 1987)

Kato et al (1989) began to experiment with different shapes in polishing with magnetic assistance. Some of the various shapes include balls, rollers, flats, internal and external surfaces. Their work focused on using magnetic fluid, as well as investigating MAF for various surfaces. They initiated investigation of using these techniques for finishing of silicon nitride. Also, they were the first to include a float within the polishing chamber for increased polishing forces, which increases the material removal rate. This is the first incarnation of the MFP process as we know it now.

2.2 Investigation of MFP and Parameters

Umehara et al (1990) were responsible for parametric study of the MFP process and how each aspect of the process affects the results. The addition of the float, and its effect on the MRR was the first of these parameters to be

investigated. Among others studied are: total grinding load, abrasive concentration, spindle speed, abrasive particle size, float stiffness, materials used in construction, and magnetic fluid.

The two main characteristics of interest are MRR during the process, and sphericity of the balls after the polishing has occurred. Each of the above listed parameters were investigated with respect to these two characterizations. When applicable, other effects of the parameter on other aspects of the process were also examined.

Adding the float to the MFP process was probably the single most significant change in the evolution of the process. The float is a thin disk of non-magnetic material than supports the balls. Surface area over which the magnetic pad acts is increased significantly, which in turn increases the grinding load that can be applied. Figure 2.3 shows the effect of the float on the magnetic buoyancy force. As the distance between the bottom of the chamber and either the float or the balls decreases, the magnetic buoyancy force increases. This compressive force is measured by the use of a dynamometer that is placed below the chamber. As can be seen, the force increases at a much more rapid rate with the float than without, resulting in a greater total buoyancy force.

This increase in compressive force should lead to an increase in MRR. By investigating this relationship at various speeds and at various grinding loads, this relationship was verified. Figure 2.4 shows the relationship between the spindle speed and the MRR, at several different loads, with and without the float.

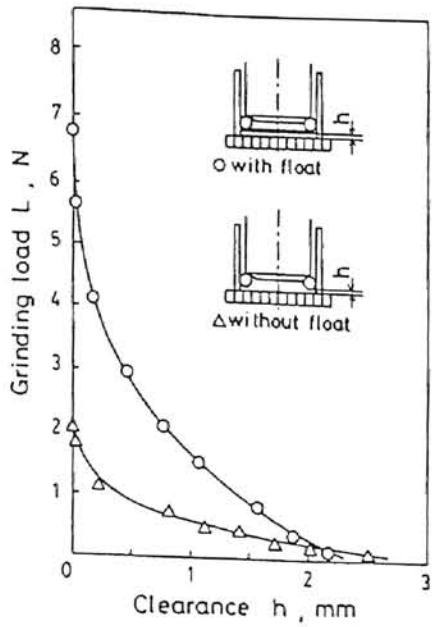

Figure 2.3 - Effect of Float on Buoyancy Force (Umehara and Kato, 1990)

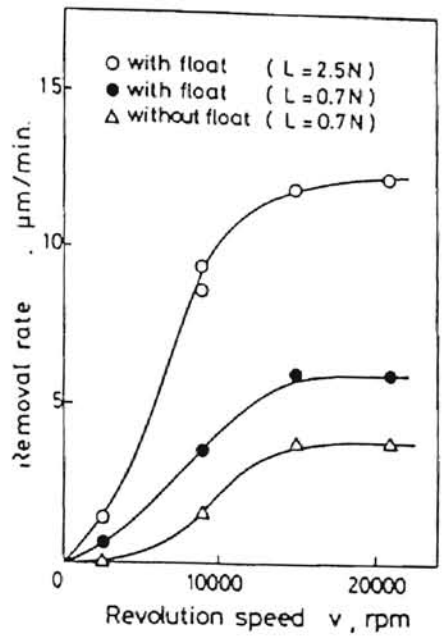

Figure 2.4 - Effect of Float on MRR at Various Speeds
(Umehara and Kato, 1990)

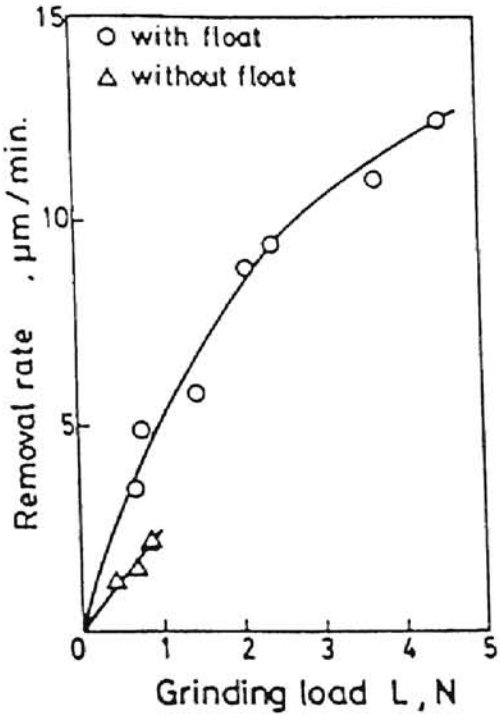

Figure 2.5 - Effect of Grinding Load on MRR (Umehara and Kato, 1990)

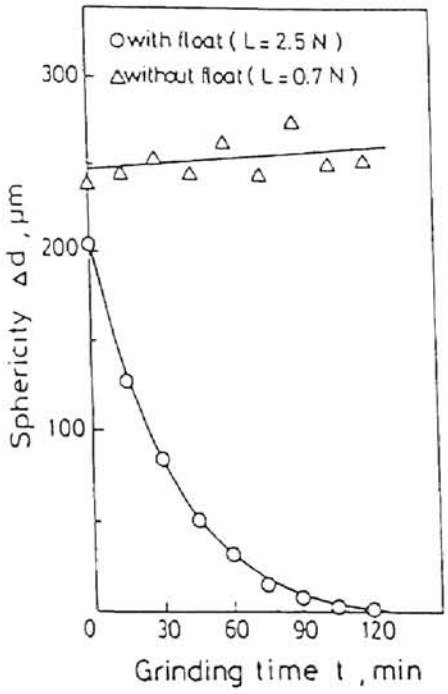

Figure 2.6 - Effect of Float on Sphericity (Umehara and Kato, 1990)

Figure 2.5 shows a direct relationship between the grinding load applied and the MRR achieved with and without the float. As expected, when the load increases, the MRR increases along with it.

Of great interest is the effect of the float on the sphericity achieved. Figure 2.6 shows the experimental results showing that the float is absolutely necessary for the MFP method to work. Without the float, the sphericity of the balls increases, and this makes the MFP process effectively useless for finishing ball bearings. In addition to better sphericity, the addition of the float also results in better surface finish.

Abrasive size and concentration are shown to have a large effect on MRR. Increases in both the abrasive size and concentration show an increase in MRR up to a point, at which the MRR either remains constant or reduces. Figures 2.7 and 2.8 show the effect of abrasive concentration and abrasive particle size on MRR, respectively.

Different materials were used by Umehara (1990) for the float, shaft and guide ring to determine how they affect the MRR. Among the materials used for the float were acrylic, urethane rubber, and silicon nitride. Removal rates for each float were similar, but the acrylic float encountered the most wear. Shaft materials tested were urethane rubber, brass, silicon nitride, aluminum, and stainless steel. Among these, the stainless steel gave the highest MRR, and the lowest amount of wear. Materials used for the guide ring include urethane rubber, stainless steel and silicon nitride, with urethane rubber giving the highest MRR and lowest wear.

The stiffness of the supporting magnetic field was taken into consideration by Umehara (1994). The magnetic field stiffness is defined as change in force

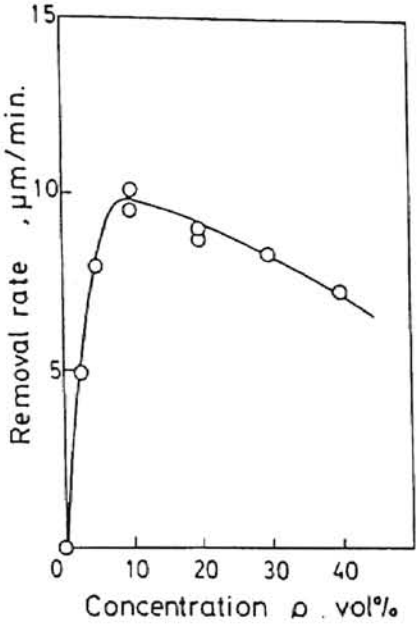

Figure 2.7 - Effect of Abrasive Concentration on MRR
(Umehara and Kato, 1990)

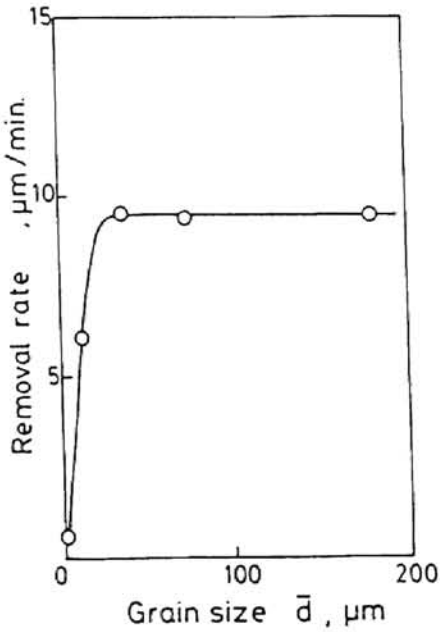

Figure 2.8 - Effect of Abrasive Particle Size on MRR
(Umehara and Kato, 1990)

per change in height within the field. Findings indicate that a lower stiffness leads to lower MRR and lower surface finish and sphericity. A higher field stiffness causes the sphericity to decrease more rapidly.

2.3 Ball Kinematics

In order to understand more thoroughly the polishing process, the study of the kinematics of the ball during the process has been carried out, both analytically and experimentally. Childs et al, (1994) were the first to analyze the ball motion. Figures 2.9a and 2.9b show the motion vectors of various components of the polishing chamber, and the forces acting between different bodies respectively.

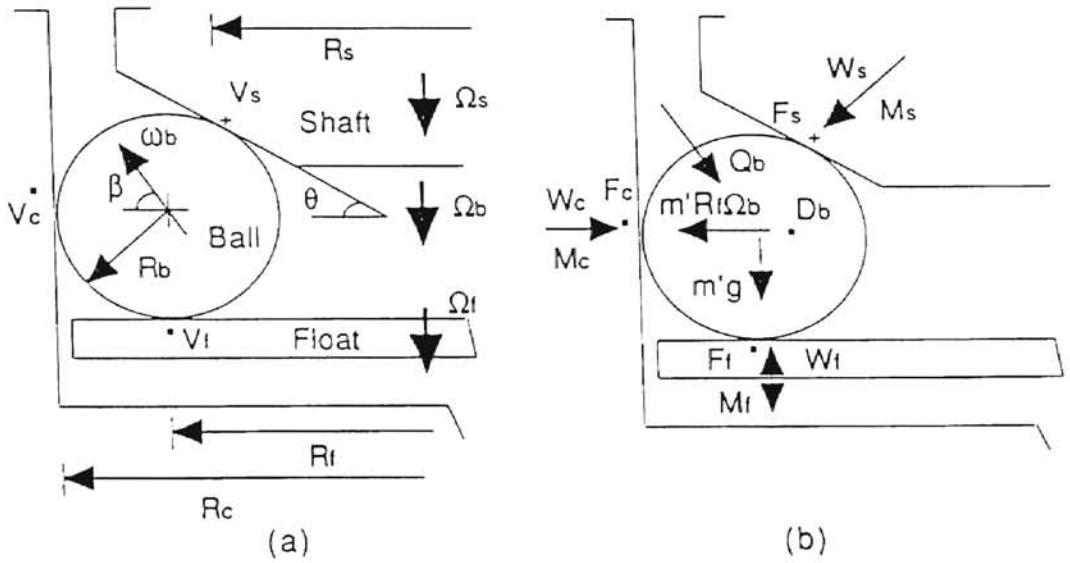

Figure 2.9a - Motion Vectors of Various Elements in MFP
2.9b - Forces Acting on the Ball (Childs et al, 1994)

where R_c = inner radius of guide ring

R_b = radius of the ball

$R_f = R_c - R_b$ = radius at which the ball contacts the float

$R_s = R_f - R_b\sin\theta$ = radius at which ball contacts the shaft

θ = chamfer angle of the shaft

β = is the angle between the horizontal and the spin axis of the ball

ω_b = angular speed of the ball

Ω_b = ball circulation speed around the guide ring

Ω_f = angular speed of the float

Ω_s = shaft rotation speed

V_c = sliding speed at contact point between ball/guide ring

V_s = sliding speed at contact point between ball/shaft

V_f = sliding speed at contact point between ball/float

Analysis of the motion produces the following relationships for V_c, V_s, V_f.

$$V_c = R_f\Omega_b - R_b\omega_b\sin\beta$$

$$V_s = R_s\Omega_s - R_f\Omega_b - R_b\omega_b\cos(\beta-\theta)$$

$$V_f = R_f\Omega_b - R_b\omega_b\cos\beta - R_f\Omega_f$$

If there is no sliding at these three points, the following relationship can be established between the ball circulation speed and the float rotation speed:

$$\alpha = \frac{\Omega_b}{\Omega_f} = \frac{R_s + R_f\dfrac{\Omega_f}{\Omega_s}\cos\theta}{R_f\left(1+\cos\theta+\sin\theta\right)}$$

If sliding is assumed to occur at the contact point between the ball and the shaft, then the sliding speed can be determined from the above based on observations of the ball circulation speed and float speed. Experimental observations were made in this manner by Childs et al at various conditions. The results of the experimentation are summarized in Figure 2.10.

Another investigation of the ball mechanics was undertaken by Zhang and Uematsu in 1996. Their investigation was targeted at the geometry used in conventional V-groove lapping, but is still applicable to our situation. Figure 2.11 shows the contact geometry of a ball under lapping conditions (similar to Figure 2.10). Figure 2.12 show how the contact trace was generated based on this geometry and knowledge of the ball motion.

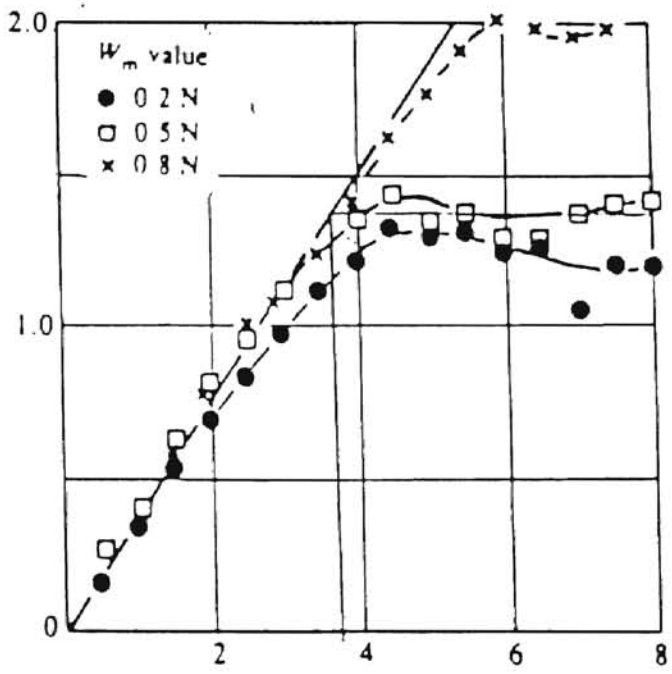

Figure 2.10 - Relationship Between Ball Rotation Speed and Shaft Speed (Childs et al, 1994)

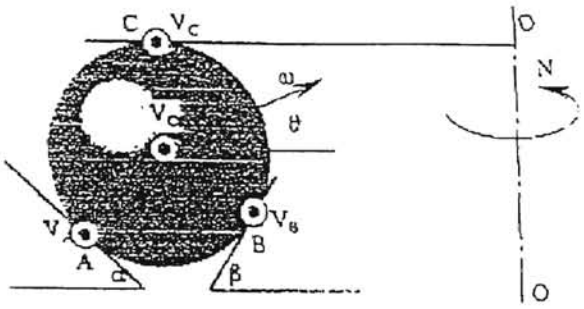

Figure 2.11 - Contact Geometry in Ball Lapping (Zhang and Uematsu, 1996)

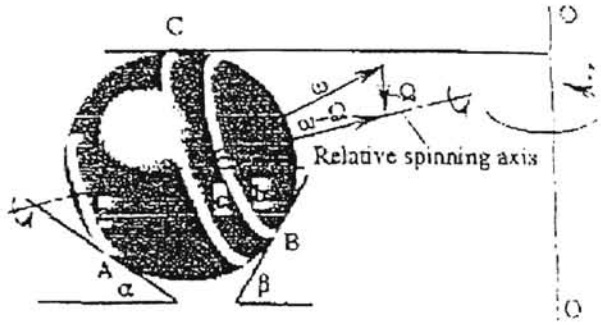

Figure 2.12 - Contact Trace Generated in Lapping (Zhang and Uematsu, 1996)

In the above figures, points A, B, and C are the points of contact, and point O is the center of the ball in consideration. The vector ω is the rotation vector for the ball, and θ is the angle that ω makes with the horizontal. Equations for the velocities at these points are as follows:

$$V_A = V_O - r\omega\cos(\alpha+\theta)$$

$$V_B = V_O - r\omega\cos(\beta-\theta)$$

$$V_C = V_O + r\omega\cos\theta$$

Re-arranging the above equations, we can solve for the spinning speed of the ball, V_O, the angle of the ω vector, θ, and the magnitude of the vector ω. The results are as follows:

$$V_O = \frac{V_A \sin\beta + V_B \sin\alpha + V_C \sin(\alpha+\beta)}{\sin\alpha + \sin\beta + \sin(\alpha+\beta)}$$

$$\tan\theta = \frac{V_A \cos\beta - V_B \cos\alpha - V_o(\cos\beta - \cos\alpha)}{-V_A \sin\beta - V_B \sin\alpha + V_o(\sin\alpha + \sin\beta)}$$

$$\varpi = \frac{V_C - V_o}{r\cos\theta}$$

Using these equations and applying the conditions seen in the lapping process, a contact trace as seen in Figure 2.12 can be generated. This information was checked by painting balls with a black paint and grinding them for short periods of time. The scratches left in the paint on the surfaces of the balls was consistent with the expected contact trace. These equations are based on the fact that there is no sliding at the contact points. We know that this is not the case seen in polishing. If the equations are modified to allow for a certain amount of slipping, then the following adjustment to the contact trace can be made as seen in Figure 2.13.

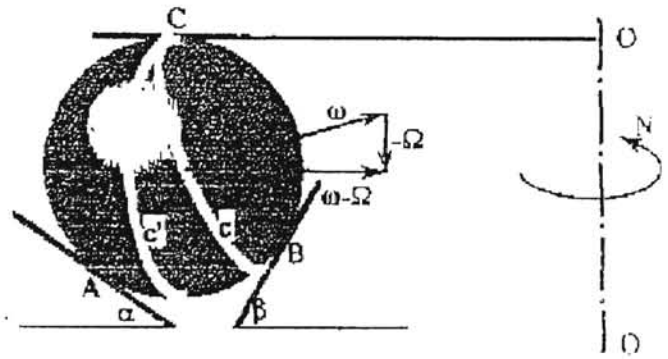

Figure 2.13 - Change in Contact Trace Due to Sliding Contact
(Zhang and Uematsu, 1996)

2.4 Variations on MFP

Some variations on the theme of MFP have been examined in the past to see how changes will affect the process. One method replaces the bank of permanent magnets with a circular electromagnetic coil. This has the benefit of

a circular shaped magnetic field being generated instead of the grid or checkerboard field generated by the permanent magnet base. Research by Dock (1995), and Cetin (1997), has shown an increased removal rate due to the use of the electromagnetic field. The figure below shows a schematic of the electromagnetic polishing chamber. One big disadvantage to the electromagnetic apparatus is its size and weight. It can be quite cumbersome to place on the mill table for polishing.

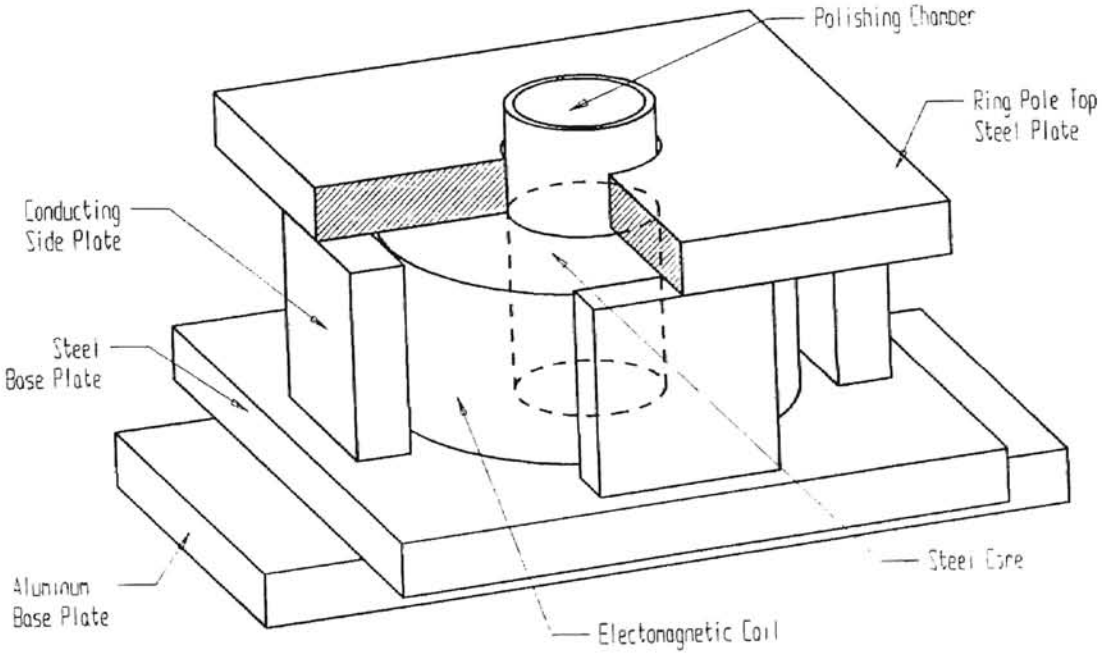

Figure 2.14 - Electromagnetic MFP Apparatus

In other research, the polishing shaft used in the MFP process was set eccentrically to the path that the balls follow around the guide ring. This method is sometimes used in V-groove lapping, and was transferred to the MFP process by Zhang et al (1996). By moving the spindle eccentric to the guide ring, the ball contact trace rotates during polishing, putting more of the ball's surface in

contact with the spindle. This results in higher MRR, and lower values for sphericity as reported by Zhang et al. Figure 2.15 shows a schematic of the eccentric apparatus used by Zhang et al.

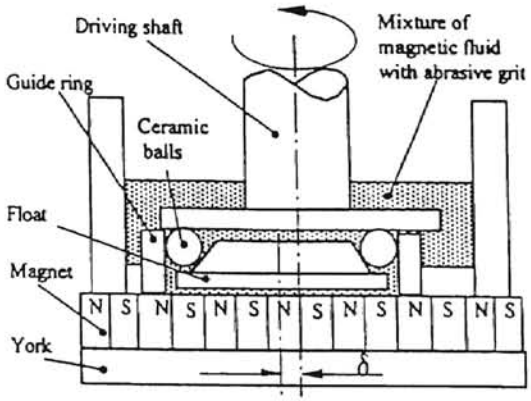

Figure 2.15 - Eccentric Shaft used by Zhang et al, (1996)

Another modification to the MFP process that has been investigated is the use of chemo-mechanical polishing during the finishing stages of the process. Komanduri et al, (1996), and Baghavatula, (1995), have both examined the possibility of using abrasives that are actually softer than the work material, but can achieve material removal due to a chemical reaction. This chemical reaction produces a softer product which can then be removed by the soft abrasive particles. This method of material removal produces virtually no sub-surface damage, which is a problem with the conventional method of polishing, which utilizes brittle fracture as the material removal mechanism. In addition, chemo-mechanical polishing produces a very good surface finish on the balls.

CHAPTER 3

PROBLEM STATEMENT

The research conducted in this investigation focused on three separate, but closely related areas of polishing. All three are methods of magnetic float polishing (MFP) with the first topic being conventional MFP, the second being MFP with an offset, or eccentric shaft, and the third is ultrasonically assisted MFP. These variations on the theme of MFP continue the ongoing search to improve the MFP process in order to make it more efficient, get better finished product, and make it more commercially viable. The following three chapters will cover each of these topics in depth.

3.1 Conventional MFP

The MFP process has been well documented to be an excellent process for finishing silicon nitride balls quickly with good results. However, the final product still falls short of the est that can be achieved by diamond lapping in terms of sphericity and surface finish. This has lead to suggestions that MFP be used as an initial 'roughing' process to quickly remove material, and use diamond lapping as the final finishing step. The thrust of the first part of this investigation is to try to improve upon this process to achieve better final results.

In addition, the project has been extended to include a ball size that has not previously been used by this research group. Past research has focused on 1/2" and 1/4" ball diameters, while the project discussed here uses 3/8" diameter balls.

Changes have to be made in order to accommodate the different ball size, and this gives a good opportunity to closely scrutinize the process, and look for ways of improvement. That is the thrust of this project - to build a new apparatus for polishing the 3/8" diameter balls, and attempt to improve the final condition of the balls in terms of sphericity and surface finish.

3.2 Eccentric Shaft MFP

Similar to the work performed by Zhang et al, (1996), the second aspect of this investigation of MFP is to include a polishing shaft whose center of rotation is offset from the center of rotation of the ball chamber. This eccentric shaft is thought to increase the amount of sliding contact the ball experiences during the polishing. Sliding contact is thought to be the mechanism for material removal, so an increase in sliding contact should result in an increase in MRR, and balls can be finished in less time. In addition, the eccentric shaft apparatus has been reported by Zhang et al, (1996) to give better sphericity of the final product.

Based on the results published by Zhang et al, (1996), an eccentric chamber is to be built, and tests run with emphasis being placed on the MRR,

the final condition of the balls in terms of the sphericity and surface finish, and the results will be compared to the proven method of conventional MFP.

3.3 Ultrasonic Assisted MFP

The third area of research involves adding ultrasonic vibration to the MFP method. Ultrasonic vibrations are used in many, many applications including ultrasonic machining, ultrasonic cleaning, ultrasonic welding, and ultrasonic detection devices. There is a vast number of ultrasonic transducers available on the market today, in any shape, size, and frequency.

Ultrasonic machining uses high frequency vibrations to excite a tool that is placed very close to the workpiece, but not actually in contact. An abrasive slurry is then added in this area between the tool and workpiece. The ultrasonic vibrations excite the slurry and cause the abrasive particles to impinge upon the work surface and remove material.

Another wide application of ultrasonic vibrations is in cleaning tanks. A cleaning solution is placed in a tank that is suspended by the rim. A transducer placed on the tank causes ultrasonic waves to propagate through the cleaning fluid. The parts to be cleaned are then placed in the solution. The ultrasonic vibrations cause the cleaning solution to cavitate and form small bubbles. These bubbles then collapse at the surface of the part, creating a small scrubbing action. The combined effect of many of these bubbles scrubbing away cleans the surface of the part.

In adding ultrasonic vibrations to the MFP process, we hope to take advantage of properties of both of these processes. Similar to the ultrasonic machining, we hope to excite the float with these ultrasonic vibrations. By adding float vibrations, the results expected are two-fold. First of all, the additional vibrations should cause impingement of the abrasive grains on the ball surface - potentially increasing the MRR. Secondly, the float vibrations should cause the float to be in intermittent contact with the balls, instead of continuous contact as in conventional MFP. This intermittent contact should result in shorter scratch lengths on the balls, and the reduced scratch length should result in better sphericity.

In addition, we may be able to take advantage of the ultrasonic cleaning principles as well. The ultrasonic vibrations should cause the fluid to form small cavitation bubbles which will collapse as in the ultrasonic cleaners. But instead of the gentle scrubbing action given by the cleaning solutions, this fluid will contain abrasive particles. Therefore, when the bubbles collapse, there will be abrasive particles impinging upon the ball surface. This should create increased material removal as well, and could possibly increase the sphericity of the balls.

In order to investigate this, an ultrasonic transducer needs to be incorporated into the conventional MFP process. By supplying ultrasonic vibrations throughout the polishing process, we can study how the MRR, sphericity, and surface finish can be affected.

CHAPTER 4

CONVENTIONAL MAGNETIC FLOAT POLISHING

While the process of MFP has been established to achieve good results in the past, we still have not been able to get results comparable to the conventional method of diamond lapping. The table below gives ANSI standards for different ball grades for bearing applications.

Table 4.1 - ANSI standards for ball bearing grades

Ball Grade	Lot Diameter Variation (μm)	Ball Diameter Variation (μm)	Sphericity (μm)	Surface Finish Ra (nm)
3	0.13	0.08	0.08	12
5	0.25	0.13	0.13	20
10	0.5	0.25	0.25	25
16	0.8	0.4	0.4	25
24	1.2	0.6	0.6	50
48	2.4	1.2	1.2	80

When a batch of balls are evaluated and graded according to these standards, the entire batch is classified according to the highest value reported in any category. For example, if a batch meets all of the requirements for a

grade 10 rating, except for surface finish gets a grade 24 rating, then the whole lot of balls is given a grade 24 rating.

In terms of the results achieved by this research group, the most difficult parameter to get desirable results with is the sphericity. Sphericity values of less than 1.2 μm have been consistently reported with the MFP process, but as you can see this gives only a grade 48 bearing. In a few instances we have been able to get sphericity results of 0.5 μm, but this still gives only grade 24 balls. Other measurements of different parameters show substantially better results especially surface finish - for which we have seen consistent results of 20 nm or less. For measuring the ball diameter, we use a digital micrometer, which has a resolution of 1 μm, therefore it is difficult to speculate about diameter variation less than that. But we believe it is safe to say that the sphericity is the limiting factor for ranking the bearing grade of the balls. As a result we are constantly striving to better the sphericity results of the MFP process.

4.1 Problems Affecting Sphericity

There are several aspects of the process that, if not done properly, can have a negative effect on the sphericity. Some of these problems have to do with the setup of the chamber with each polishing, others have to do with chamber construction, and still others have to do with the process itself. Figure 4.1 shows how improper setup of the chamber can severely affect the motion of the balls during polishing, and therefore affect the sphericity. Figure 4.1a shows

the proper setup of the chamber with everything parallel and concentric. Figure 4.1b shows a problem that can occur during mounting of the polishing shaft to the drive spindle. This only happens occasionally, and is not a concern every time you polish. Due to the high material removal rates and large amount of sliding contact between the balls and the shaft, the shaft itself will experience large amounts of wear on the contact surface, and will acquire a radius similar to the ball radius. Periodically, the shaft is removed, and re-machined to get a flat polishing surface. When the shaft is re-mounted to the drive spindle, great care must be used when aligning the shaft axis with the drive axis.

Figure 4.1c shows how the process can be affected if the polishing shaft's drive axis is set at an angle to the polishing chamber. This is mainly a concern if and when the polishing spindle is removed from the machine tool and has to be re-mounted. Barring any damage to the spindle this should rarely occur. Another way this tilting of axes can occur is if the chamber is not mounted securely to the machine tool table. This can be prevented by taking care each time you polish to ensure that the mounting screws are flush and tight.

The third problem, and probably the most frequent, is shown in Figure 4.1d. This shows the chamber being mounted eccentric to the polishing shaft axis of rotation. This problem can occur every time the chamber is used and extreme scrutiny must be used to inspect the setup for this problem. In both cases of axis tilt and axis offset, the ball path around the chamber is severely affected as well as the sphericity of the balls.

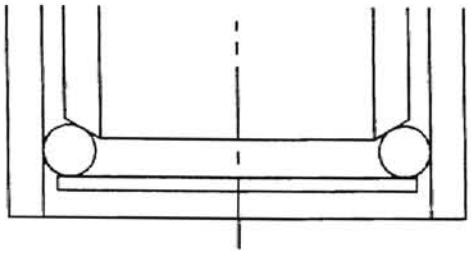

Figure 4.1a - Proper Alignment

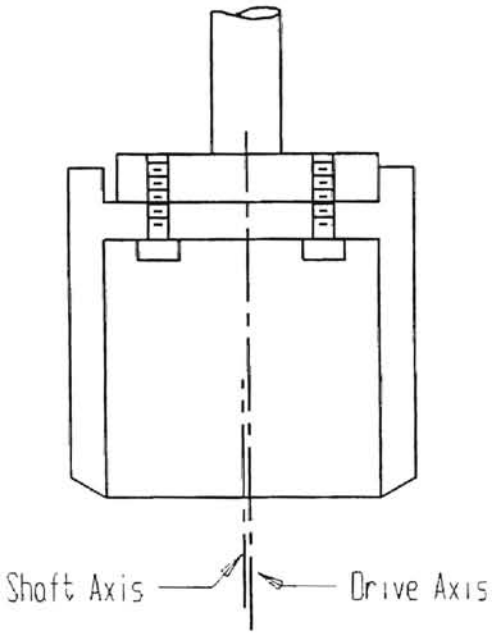

Figure 4.1b - Shaft Mounting Offset

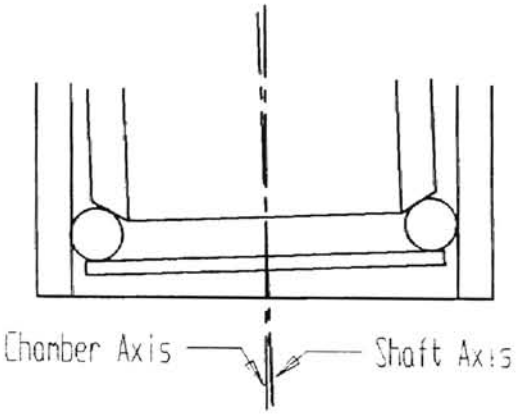

Figure 4.1c - Drive Axis Tilt

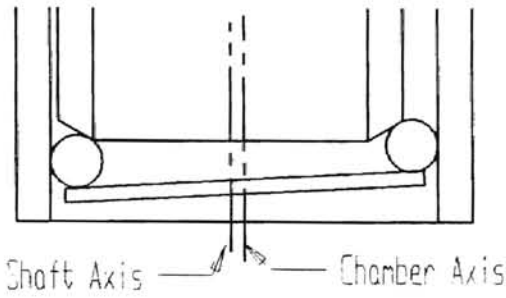

Figure 4.1d - Chamber Offset

Other areas of concern are related to the construction of the chamber, and the materials used. Great care can be taken to align the chamber so that its axis of rotation is perfectly parallel and concentric with the drive shaft axis, but this can be all for naught if either the chamber or the polishing shaft are out of round. As a result the polishing shafts that are used are manufactured elsewhere in machine shops that can machine to higher tolerances than we are able. But the chambers themselves are made in the lab by research assistants. As a result some error can be introduced during construction of the chamber. Take for example a chamber that is actually an elliptical shape instead of circular as shown in Figu e 4.2 below. This will result in the balls only contacting

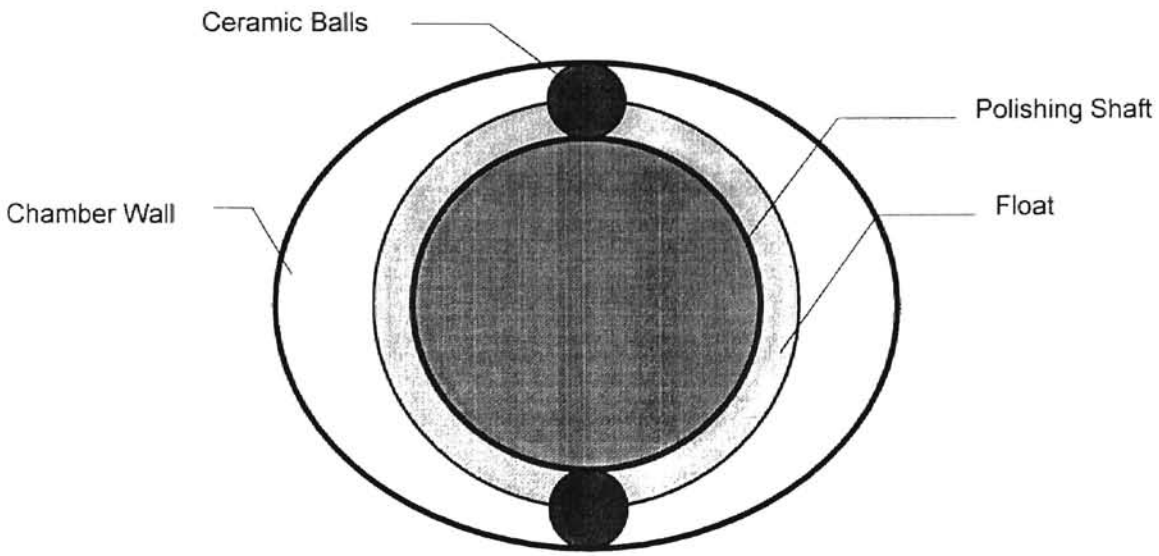

Figure 4.2 - Elliptical Polishing Chamber

all three surfaces (chamber wall, shaft and float) in two points - at the apexes of the minor axis of the ellipse. At all other points, the balls will only be in contact

with the chamber wall and the float. This eliminates the sliding contact between the shaft and balls where the material removal takes place, and as a result the material removal rate will suffer tremendously, as well as the sphericity.

Another aspect of chamber construction to consider is the uniformity of the wall thickness. A non-uniform wall thickness can contribute to both the out-of-roundness of the chamber as well as the eccentricity of the drive axis and chamber axis. The problems with chamber out-of-roundness are discussed above, but assume that the wall thickness is not uniform, and the I.D. and O.D. of the chamber are both perfectly round. This results in the following situation shown in Figure 4.3.

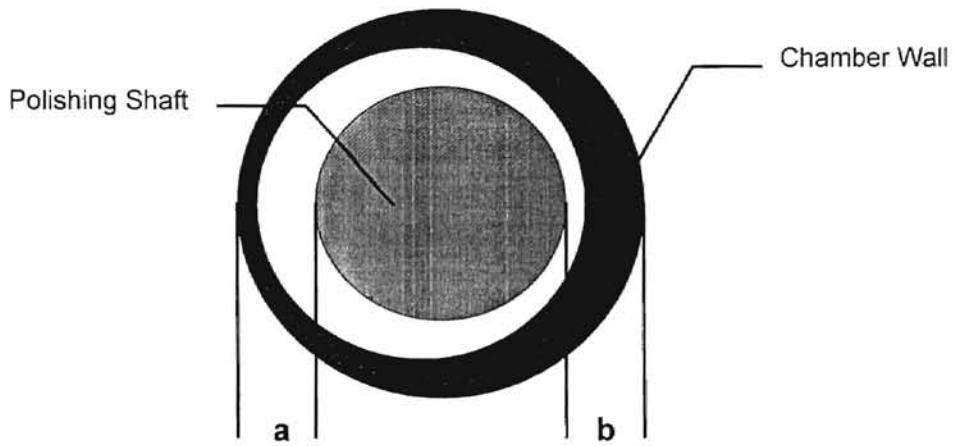

Figure 4.3 - Non-Uniform Wall Thickness

When the chamber is set up for polishing, the shaft is centered in the chamber body by measuring the distances a and b as shown above. When these two distances are equal, the chamber is properly centered. But, as you can see in the above figure, if the wall thickness is not uniform, the distances **a**

and **b** can be equal, and the polishing shaft is offset or eccentric. This situation assumes that the I.D. and O.D. are perfectly round, but not concentric. In reality, if the wall thickness is not uniform, it is very likely that the chamber is out-of-round also, resulting in a combination of effects seen in both Figures 4.2 and 4.3.

4.2 Approach

In addition to these problems associated with the physical aspects of the chamber, there are also considerations of the process itself, such as spindle speed, abrasive type and size, load applied, etc. In this aspect of the investigation, we look at these various parameters and how each can be improved while applying the MFP process to a new ball size, namely 3/8".

The effects of process parameters are quite well documented, as seen in Chapter 2. As a result, these are assumed to be well established and not worth close investigation. The problem left in relation to the 3/8" balls is mainly chamber design and construction. We want to keep as many things similar as possible, for easy incorporation, while changing the aspects that we believe will result in better sphericity.

4.3 Equipment Design

When allowing for the different size of the ceramic balls, a few things have to be considered. For example, the chamber diameter can remain the same, and the polishing shaft can increase in diameter to accommodate the change

from 1/2" to 3/8" balls. The other alternative is to construct a new chamber, and keep the same polishing shaft. Given the fact that we already posses several polishing shafts of the same geometry, and very high tolerances, it makes more sense to construct a single chamber one time, than having to worry about having two different shaft sizes that will have to be changed any time another ball size is needed. As mentioned previously, removing and re-mounting the polishing shaft is quite time consuming, as great care has to be taken to ensure a concentric mount. This, along with the fact that the chamber is removed for cleaning between every polish, makes it obvious that a new chamber is the most efficient method to accommodate the new ball size.

Now that this question has been answered, the next topic to tackle is the materials to be used for the new chamber. During chamber construction is the ideal time to consider avoidance of the problems of chamber out-of-roundness, and wall thickness variance as discussed previously. Indeed, one would be lax in their duties as an engineer not to consider such things.

Previous chambers have used an acrylic tube as the chamber. This was pressed into an aluminum base that had been machined on a CNC mill in order to mount to the transducer. This acrylic tube in undoubtedly extruded into its final shape. The only machining done on the tube was the addition of a chamfer on the end to facilitate pressing it into the aluminum base. This leaves the possibility of any out-of-roundness or wall thickness variation wide open. In order to eliminate the possibility of this, we opted to machine the chamber for this project out of a solid piece of aluminum.

To preserve dimensional integrity of the aluminum workpiece, all machining was done without ever removing the workpiece from the lathe chuck. This eliminates any possibility of centering error when the piece is re-mounted. In addition, great care was taken to get good dimensional stability, and good surface finish on the machined surfaces. The figure below shows how the machining occurred, and while this did result in much more waste material, it is a one time process, and the extra material used is well worth the added benefit of good dimensional control. Figure 4.4 below shows how the chamber was machined while never needing to remove the workpiece.

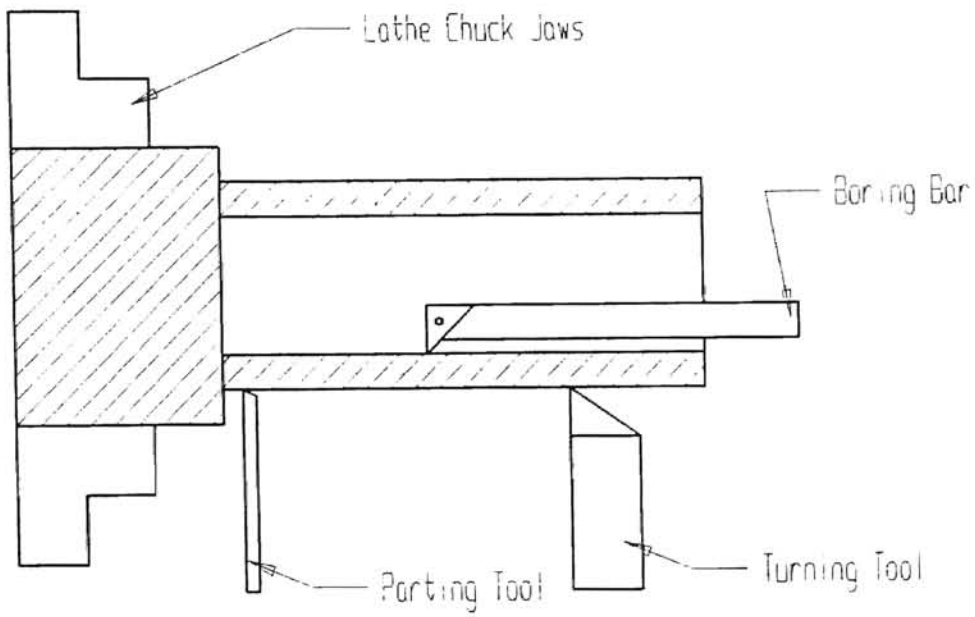

Figure 4.4 - Machining Process for New Chamber

By machining the chamber in this manner, we can be assured of better geometrical stability in terms of concentricity, wall thickness, and the perpendicularity of the end surfaces with respect to the chamber walls.

This chamber was used with a base that had been machined on a CNC controlled mill, which has very good dimensional tolerances. Fitting the chamber into the base was done with great care to ensure that the chamber walls will be perpendicular to the chamber base. The exterior of the chamber was shimmed with tape in order to achieve a snug fit into the base.

4.4 Tests Run

Now that the chamber has been constructed, tests need to be run in order to determine whether the new construction has any effect on the finished product. In particular, we are looking for an improved sphericity, with no degradation of the other parameters. The test were conducted on a fresh batch of balls - that is the initial condition of the balls is as they are received from the supplier. There has been no previous polishing performed on them.

The polishing process is divided into three basic steps: rough grinding for high MRR, fine polishing for good sphericity, and finishing for good surface finish. The first stage is basically to reduce the diameter of the balls and remove the band that is present at the center of the balls, as shown in Figure 4.5. This band is due to the geometry of the molds used to compact the ceramic powder into the desired shape. Also, this rough grinding serves to improve the sphericity of the

balls as well. Often times a sphericity of about 1-2 μm can be seen in this stage. Once the balls are within about 100 μm of the final diameter, the fine polishing is implemented to further improve the sphericity, and

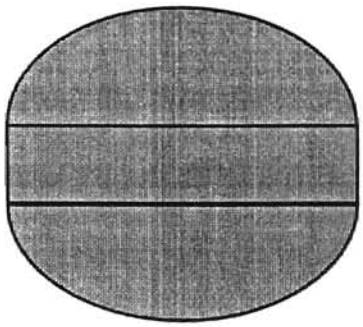

Figure 4.5 - 'As Received' Condition of Ceramic Balls

accurately approach the target diameter. Once a good sphericity is achieved, and the balls are within a few micrometers (oversized) of the final diameter, the finishing stage begins. In the finishing stage, the MRR is negligible, and has little or no effect on the sphericity or diameter. Often this finishing stage implements chemo-mechanical polishing, in which abrasives are used that are actually softer than the work material, but due to a chemical reaction, the material is softened on the surface allowing the softer abrasive to mildly remove material. This results in a very high surface finish quality.

As expected the rough machining uses larger and harder abrasive particles and the fine polishing uses incrementally smaller and softer particles. The finishing stages use very small abrasive particles - usually < 1μm - in order to get good surface finish.

Experiments were conducted in this manner. Rough grinding was performed until the balls were within about 100 μm of the final diameter. At this point, smaller and softer abrasives were used until the final diameter was reached, and then the finishing took place. Measurements of MRR and sphericity were taken throughout the process to characterize the balls, and surface finish measurements were added at the final stages for evaluation. Table 4.2 below gives the conditions used during polishing tests performed during this investigation.

Table 4.2 - Polishing Conditions

Work Material	HIP'ed Silicon Nitride
Abrasive Type	B_4C, SiC, Cr_2O_3, CeO, Al_2O_3
Abrasive Size	>1 - 40 μm
Abrasive Concentration	5 - 10% by volume
Ferrofluid	W40 - water based fluid
Magnets	Rare Earth Magnets (Nd-Fe-B) Size: 1/4" x 1/4" x 1/2"
Load	0.5 - 1.5 N/ball
Spindle Speeds	1000 - 4000 rpm
Machine Tool	PI Air Bearing Spindle Bridgeport CNC Milling Machine
Polishing Time	15 - 120 minutes

Polishing times for each test are typically kept at about 45 - 60 minutes. This limitation is present due to the fact that the water tends to evaporate out of the fluid as the polishing occurs, due to heat generated by friction. The range of 45 - 60 minutes seems on the safe side of this problem for most conditions. In extreme cases, such as very high speeds with large abrasives, we may polish for shorter times. Also, in the finishing stages, very little material is being removed, therefore, very little heat is generated, and the polishing time can be extended up to 120 minutes. Often, when the balls are near the target diameter, only a very small amount of material needs to be removed, and through calculations based on the MRR data, we can predict how long the test needs to run in order to remove the desired amount of material. Sometimes this requires a polishing time of only 15 - 20 minutes. This is the reasoning behind the choice of polishing times for each test.

Abrasive concentration is chosen based upon previous work by Umehara and Kato (1990). They found that MRR increased with an increase in abrasive concentration up to about 10% by volume. Beyond this point, additional abrasive particles actually serves to decrease the MRR. Figure 2.7 in Chapter 2 gave a graphical representation of this trend. In addition, discussion of results with my colleagues seems to indicate that an abrasive concentration of 5% gives better sphericity results than an abrasive concentration of 10%. Therefore, when high MRR is required, a concentration of 10% is used, and when sphericity is a concern, the abrasive concentration is reduced to 5%.

4.5 Experimental Results

Two different batches of balls were processed with the new chamber. The first batch was started in the "as received" condition, but were not finished completely. The second batch had been previously polished, but 375 μm of extra material were left - which is plenty to establish the validity of the chamber.

4.5.1 Batch #1

As stated previously, the balls for batch #1 were started in the "as received" condition. The tests run are summarized in Table 4.3 along with any measurements made after each run.

At this point in the testing, the balls were within 85 μm of the final diameter. As can be seen below, the last two test were run with B_4C-800 as opposed to B_4C-500. This is the first step in the gradual reduction of abrasive size and hardness seen in the fine polishing stage. Also of great importance are the sphericity measurements taken at after the last test. The value of 0.63 μm for sphericity is a very comparable result with the previous conventional polishing chambers built for different size balls. The difference being that the good sphericity was achieved here in the rough grinding stage, where results this good are often seen in the other chambers only after the fine polishing stage. This indicates one of two things: either the ball diameter is optimal for this size

chamber, or the extra effort put into the chamber construction paid off with good results.

Table 4.3 - Batch #1 Test Runs

Run #	Abrasive	Spindle Speed rpm	MRR mg/ball/min	Sphericity μm	Time minutes
1	B_4C -500	2000	-	-	60
2	"	"	0.205	-	60
3	"	3000	0.791	-	50
4	"	"	0.497	1.08	60
5	"	"	0.739	-	60
6	"	"	0.727	1.26	60
7	"	"	0.537	-	55
8	"	"	0.493	-	55
9	"	"	0.217	0.73	60
10	B_4C-800	2000	0.028	0.91	60
11	"	"	0.492	0.63	60

4.5.2 Batch #2

At this point another batch was started with the chamber to check repeatability of the results. The balls used in this batch had already been polished some, as stated previously, but still had plenty of material left for all three stages of polishing. Initially, there was about 375 μm of material left on the balls to be removed. Again, each test run is summarized below in Table 4.4 with similar information as above.

The initial sphericity of these balls was approximately 0.7 μm. Again the rough grinding showed great promise with excellent sphericity results of 0.47μm,

after only a few hours of grinding. This is better than previous attempts with other chambers. But notice that the sphericity increases as further polishing is

Table 4.4 - Batch #2 Test Runs

Run #	Abrasive	Spindle Speed rpm	MRR mg/ball/min	Sphericity μm	Time minutes
1	B_4C -500	3000	0.780	0.50	75
2	"	"	0.667	0.47	75
3	"	"	0.688	0.85	45
4	SiC-1000	"	0.633	1.00	30
5	SiC-1200	"	0.183	-	60

carried out. Contrary to expectations, as the abrasive is changed to SiC -1000, which is both smaller in size and softer than B_4C - 500, the sphericity actually increases to a value of 1 μm. The final test again changes abrasive to an even smaller size, but there was no significant change in sphericity, and by this time the balls were under the target diameter of 9.525 mm (3/8") by ~0.003 μm, so no further testing was done with this batch.

4.5.3 Batch #3

Since the previous two batches have showed very good results during the rough grinding but poor results in the fine polishing stages, the third batch focuses on the fine polishing, and finishing of the balls. A batch of balls was used that had previously undergone a lot of polishing, and were near the target diameter. This particular set has about 38 μm of material left, and a sphericity of

2.54 μm. Often times in the rough grinding stage over 100 μm of material can be removed in one hour of polishing, so there s clearly no room for rough grinding with this batch. We are forced to start with the fine polishing stage to attempt to improve the sphericity. Table 4.5 below gives the data for this batch of balls.

Table 4.5 - Batch #3 Test Runs

Run #	Abrasive	Spindle Speed rpm	MRR mg/ball/min	Sphericity μm	Time minutes
1	SiC-1200	3000	0.192	1.12	60
2	SiC-8000	"	0.022	1.22	50
3	B_4C-1500	"	0.028	1.16	60
4	"	"	0.012	1.38	55
5	SiC-1200	"	0.047	1.26	15
6	"	"	0.054	1.15	25
7	"	"	0.022	1.18	35
8	"	"	0.194	-	25

The initial jump in sphericity is very good - from 2.54 μm to 1.12 μm. Unfortunately this trend does not continue as the abrasives are changed. After tests 2,3, and 4 did not improve the sphericity, SiC -1200 was used again, due to the fact that this particular abrasive was responsible for the initial improvement in sphericity. But, as can be seen, no further improvement occurs.

One other point of interest arising from the above data is the MRR of the SiC - 1200 abrasive. Note that the first test shows a MRR of 0.192 mg/ball/min, yet subsequent tests return much lower MRR's of 0.047, 0.052, and 0.022

mg/ball/min. These results are consistent with other tests in which this particular abrasive was used. During the final test, the MRR again jumps up to 0.194 mg/ball/min. This unpredictable nature of the abrasive makes it very difficult to accurately approach the target diameter. Indeed, due to this extreme jump in MRR, the balls ended up being significantly under the target diameter.

One possible explanation for the difference in MRR is that there were large abrasive particle embedded in the polishing shaft from previous polishings. This sort of particle embedding is known to happen, and could explain why the first test had such a high MRR - there were larger abrasive particles present than was intended. But, this theory will not explain why the final test shows a similar jump. The three previous tests all used the same abrasive, and gave similar MRR's, so there could not be any large particles embedded from these tests. This strange behavior is very difficult to explain.

4.6 Discussion

The new chamber constructed does show some promise for polishing the 3/8" diameter balls. Tests performed with large abrasives in the rough grinding stages gave MRR's as expected - that is to say, very similar to the other conventional polishing chambers used for different sizes. Sphericity measurements during this rough grinding stage showed a noticeable improvement over the other chambers.

Previously an average sphericity of 0.6 μm was considered good for a batch of balls finished with conventional MFP. The new chamber was built from the beginning with precision in mind. Apparently this attention to accuracy during the construction phase is justified due to the improved sphericity of 0.47 μm seen with this chamber.

There is however a problem seen in the finishing of these three batches of balls. This problem lies in the fact that these good values of sphericity could not be maintained through the fine polishing and finishing stages. When smaller and softer abrasives were used, the sphericity suffered. This is contrary to all of the previous work done on MFP of ceramic balls.

Since these results are so different in nature, one looks for indications why this is happening. Initial investigation leads us to look at differences between this process and previous ones. Only two things differ - first of all, the chamber itself is different, and secondly, the ball size is different. All other aspects of the process are identical to the MFP carried out in the past: the magnet base, the magnetic fluid, the polishing shaft, the machine tool, the abrasives, etc. Since only two things differ, one of these, or a combination of these new parameters and one or more of the others is causing the poor final results.

On the other hand, the chamber showed very good results with the large abrasives on the new ball size. It is only when we switch to the smaller abrasives that the sphericity increases. This leads us to suspect the abrasives

themselves. But again, these very same abrasives were used previously with very good results. The bottom line is that it is very difficult to pinpoint the problem without further investigation.

If we focus on the main thrust of this investigation, we can see that there was some progress made. The accuracy of the chamber during construction was improved in the attempt to better the sphericity results. This goal seems to have been achieved due to the low sphericity values during the roughing stages. There appear to be some process related problems preventing these good sphericity results from being carried through to the finishing stages.

CHAPTER 5

ECCENTRIC SHAFT MAGNETIC FLOAT POLISHING

It is known that the sliding action between the drive shaft and the ceramic balls is responsible for material removal (Childs et al., 1994). Abrasive particles are embedded into the shaft, creating a two-body abrasion situation. Based on this information, one would assume that an increase in sliding contact will give an increase in material removal rate (MRR). Following this line of logic Zhang et al. (1996) first conceived the idea of moving the axis of rotation of the polishing shaft eccentric to the axis of rotation of the chamber. This eccentricity will without a doubt cause an increase in sliding contact. In addition to a higher MRR, Zhang et al. (1996) also report that an decrease in sphericity values was seen with the eccentric apparatus. In order to investigate this aspect of MFP, an eccentric shaft polishing apparatus was built and tested.

5.1 Approach

The research conducted by Zhang et al. (1996) was based on contact trace theory proposed by Zhang and Uematsu (1996). This work evaluated the point of contact between the polishing shaft and the ball both by calculation and experimental observation. By setting the polishing shaft eccentrically, this

contact trace is rotated around the ball. In order to get the contact trace to cover the entire surface of the ball, it needs to rotate through 180^0. This corresponds to half of the perimeter of the ball which is equal to one half of the amount of eccentricity. In other words:

$$\pi R_b = 2\delta$$

where R_b is the radius of the ball and δ is the amount of eccentricity. This equation reduces to:

$$\delta \approx 1.6\ R_b$$

The following figure shows a graphical representation of how the contact trace of the ball changes with eccentricity.

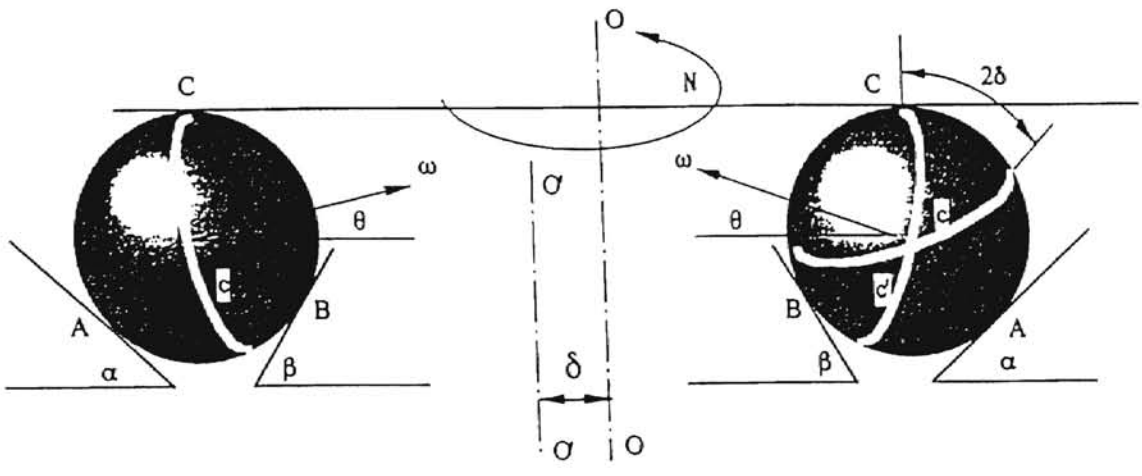

Figure 5.1 - Contact Trace Change with Eccentricity (Zhang et al., 1996)

5.2 Equipment Design

We want to design and construct a chamber based on this contact trace theory, but scale the chamber up for 1/2" ball diameter. Another design criteria to consider is the batch size, or how many balls can be polished at one time. Other chambers are capable of polishing 12-14 balls per batch, and we wanted to carry this over for this new chamber. In order to accomplish this, we needed a guide ring of about 3" in diameter. By applying the equation above (Zhang et al. 1996) we can determine that for 0.5" diameter balls we will need an eccentricity of 0.4". This leads to the determination of the shaft diameter, as shown in the figure below.

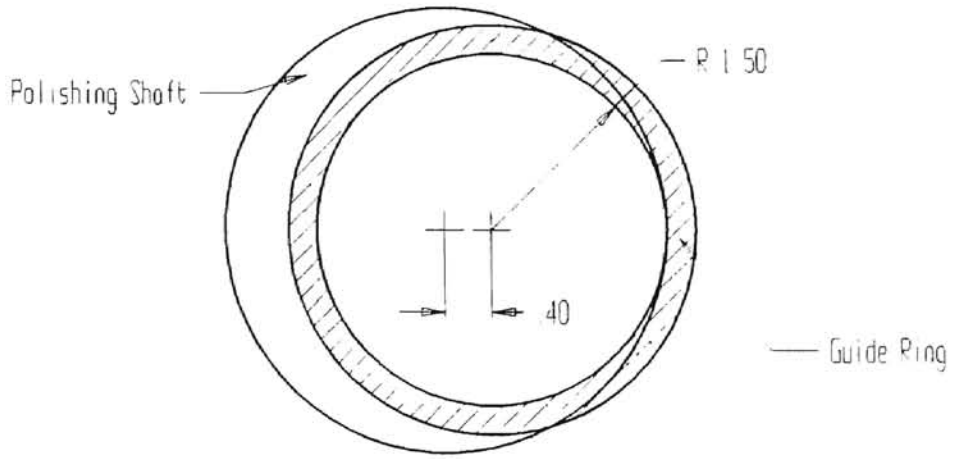

Figure 5.2 - Eccentric Shaft Radius Calculation

One can see that the radius of the polishing shaft needs to be the radius of the guide ring plus the amount of eccentricity desired. In this case the guide ring is 1.5" in diameter, and the eccentricity is 0.4" which gives a shaft radius of

1.9". This was rounded up to 2.0" to give a margin of error while manufacturing, and to give a little bit of overhang to ensure the ball stay contained within the guide ring.

Now that we have the essential parts of the chamber designed, the rest of the chamber is basically built to fit around these components. The following two figures, 5.3 and 5.4, show a schematic of the assembled chamber, and an exploded view of the chamber with dimensions on each component, respectively.

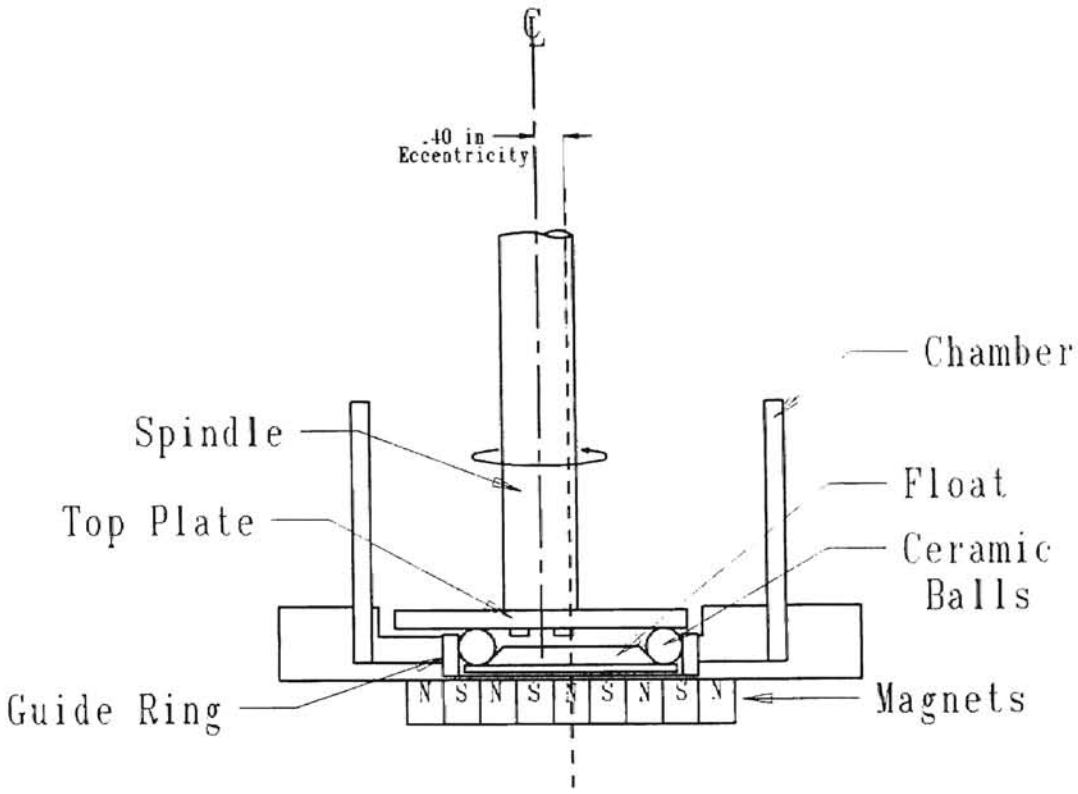

Figure 5.3 - Eccentric Shaft Polishing Chamber

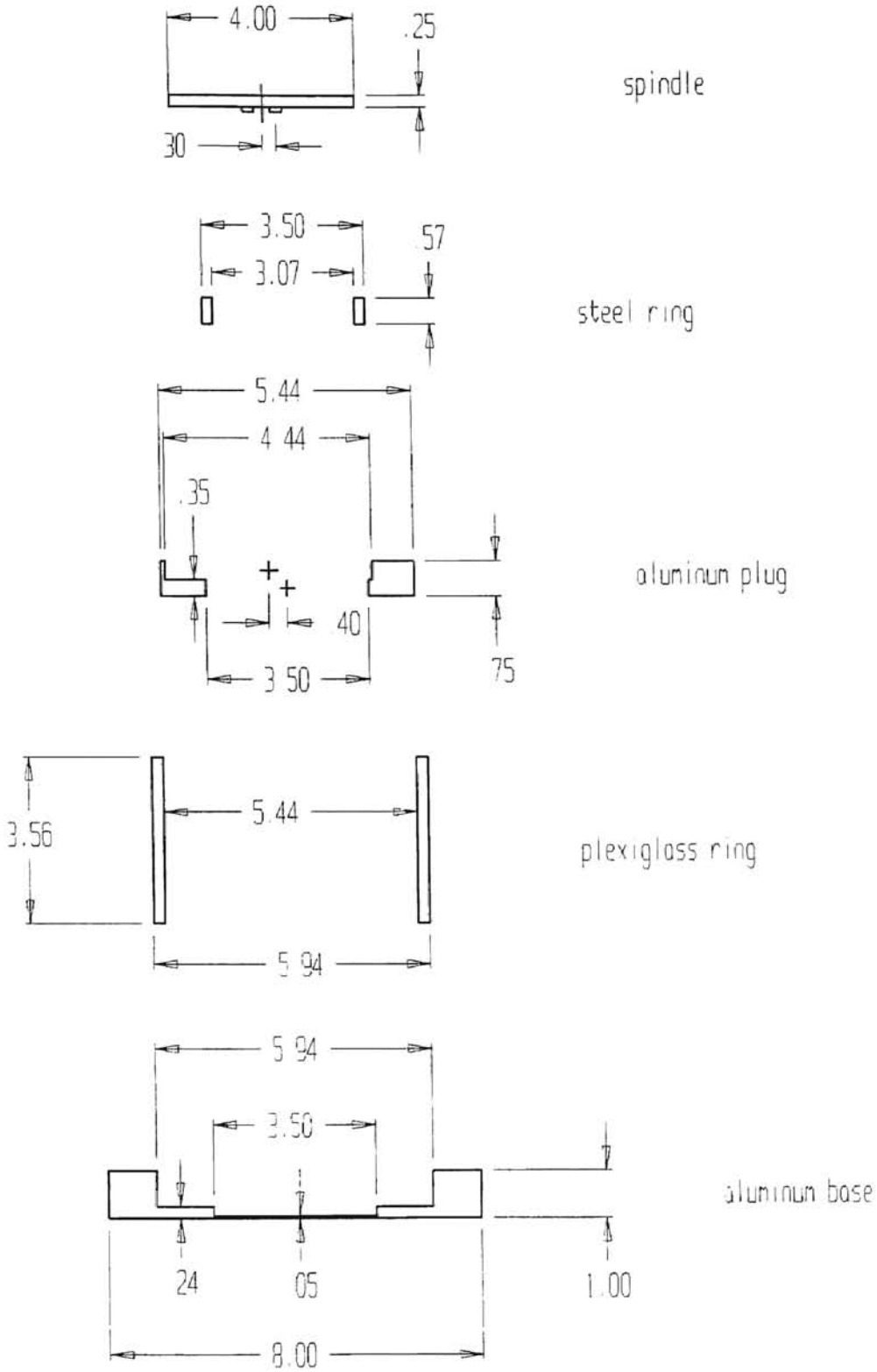

Figure 5.4 - Exploded View of Eccentric Chamber

The main difference between this chamber and the one used by Zhang et al. (1996), aside from the size difference, is the inclusion of an aluminum plug around the guide ring. The purpose of this plug is to occupy space that would normally be filled with magnetic fluid. This design modification allows us to use much less fluid in order to submerge the balls, and due to the high cost of the fluid, this represents a large savings. In addition, this keeps the abrasive particles concentrated in the machining area, instead of flowing outside of the guide ring, and settling at the bottom of the chamber away from the balls.

5.3 Experiments Run

A new batch of balls was used to begin the testing of the chamber in order to evaluate how it performed during all stages of polishing - from the initial roughing stages with high MRR to the final end stages where sphericity and surface finish are primary concerns. Testing conditions are the same as those listed for the conventional grinding apparatus. For accurate comparison, the results of the eccentric shaft apparatus will be compared to conventional MFP finishing of 1/2" balls as opposed to the 3/8" balls detailed in Chapter 4.

Two different batches of balls were finished with the eccentric chamber. The experiments will be outlined in this manner, starting with the first batch. Ultimately, we want to compare the MRR and sphericity results from this chamber to those of the conventional chamber.

5.3.1 Batch #1

Tests in this batch are basically divided into three different sections: roughing stage for high MRR, fine polishing stage for good sphericity, and finishing stage for surface finish. The abrasives used in the final stage remove a negligible amount of material, and therefore have a negligible effect on sphericity. The experiments run are grouped below in Table 5.1 along with pertinent data about each test.

Table 5.1 - Batch #1 Experimental Data

Run #	Abrasive	Spindle Speed rpm	MRR mg/ball/min	Sphericity μm	Time minutes
1	B_4C - 500	1000	0.828	-	45
2	"	"	0.337	-	"
3	"	"	0.464	-	"
4	"	2000	1.8	-	"
5	"	"	1.347	-	"
6	"	"	0.798	-	"
7	"	"	1.20	-	"
8	"	"	1.176	-	"
9	"	"	1.09	-	"
10	"	3000	1.73	4.9	"
11	"	"	1.458	5.31	"
12	"	"	0.870	3.18	"
13	"	"	0.866	3.67	"
14	SiC - 1000	2000	0.479	1.61	"
15	"	"	0.17	1.54	"
16	"	"	0.29	1.68	"
17	"	"	0.36	1.8	"
18	"	"	0.42	2.1	"
19	SiC <1μm	"	0.05	2.1	"
20	CeO <5μm	"	0.003	1.91	120

Tests 1 - 13 are the roughing phase of the polishing, tests 14 - 18 are the fine polishing, and test 19 and 20 are the final finishing of the balls. Also note that the tests were run at various spindle speed in order to establish the effect that spindle speed has on MRR.

The information that is most valuable from these tests are the higher material removal rates achieved from this apparatus. Table 5.2 below summarizes the tests for different abrasives at different speeds.

Table 5.2 - MRR Data Summary

Abrasive	Spindle Speed	Average MRR
B_4C - 500	1000	0.543
B_4C - 500	2000	1.23
B_4C - 500	3000	1.23
SiC - 1000	2000	0.343

The MRR at 2000 rpm for the B_4C - 500 abrasive is notably higher than the MRR at the same conditions for the concentric chamber. This increase is expected, although it does fall short of the 3 fold increase seen by Zhang et al. (1996).

Other points of interest are the final condition of the balls in term of sphericity and surface finish. The best results for sphericity with this batch are an average batch sphericity of 1.544 μm. This falls quite short of the usual result of ~0.6 - 0.7μm for the concentric apparatus. Also note that with an increased

amount of accumulated polishing time, the sphericity does not seem to decrease as expected, but actually increases (worsens). Again this is not the expected result for this new chamber.

Surface finish measurements taken at the end of the final polishing stages showed results of 35.4 nm Ra. Again this is not up to the expectations, as it is worse than the results of ~15 - 20 nm seen from the concentric apparatus.

5.3.2 Batch #2

A new batch of balls were started as the previous batch had reached the target diameter. Again similar tests were run as with the first batch, but some different parameters were checked for comparison. Of particular interest are the tests run at the end during which the amount of eccentricity of the drive shaft was altered, and the effect of this on MRR and sphericity was noted.

Initially, the balls were rough machined with larger abrasives, and the MRR was monitored. The roughing tests are listed below in Table 5.3. The first seven test that are run use a smaller abrasive than normally used for the roughing stage, but at the time we were out of the larger B_4C - 500 abrasive. Starting with run #8, the usual abrasive is used, and tests are run at different speeds in order to determine the effect of speed on MRR and sphericity. The data for these tests is combined with the data at different speeds from batch #1 to get Figure 5.5. All other parameters are the same between batches #1 and #2.

Note that the sphericity of the balls has improved from 144 μm to about 5 μm. While this is a significant improvement, it still falls short of the desired results of <1 μm sphericity. Because of this, and due to the fact that the material removal rates are very consistent, the following tests are done in an attempt to "fine tune" the eccentric chamber, and get better sphericity.

Table 5.3- Batch #2 Rough Grinding

Run #	Abrasive	Spindle Speed rpm	MRR mg/ball/min	Sphericity μm	Time minutes
1	B_4C - 800	2000	0.472	144.9	45
2	"	"	0.487	125.39	"
3	"	"	0.490	109.7	"
4	"	"	0.616	121.9	"
5	"	"	0.684	83.15	"
6	SiC - 400	"	0.344	75.01	"
7	"	"	0.374	77.98	"
8	B_4C - 500	"	0.888	38.38	"
9	"	"	0.691	29.66	"
10	"	3000	0.734	21.28	"
11	"	"	1.297	12.21	"
12	"	"	1.019	7.3	"
13	"	4000	0.998	3.81	"
14	"	"	0.863	4.43	"
15	"	"	0.706	4.49	"
16	"	2000	0.89	4.2	"
17	"	1000	0.492	5.08	"

For the first few tests, the guide ring in the chamber was modified slightly. Previous polishings had resulted in a strange wear pattern on the urethane rubber lining that protects the guide ring. This wear pattern appeared to be a

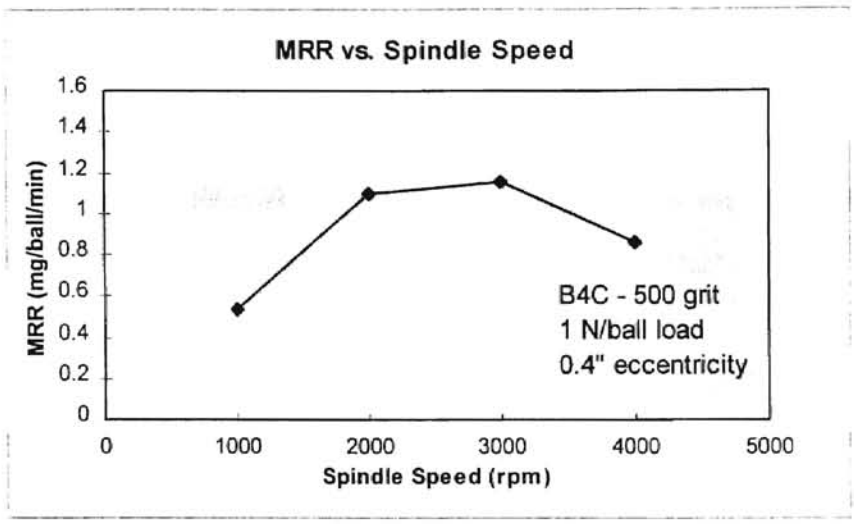

Figure 5.5 - MRR for Various Spindle Speeds

scalloping pattern or a linear arrangement of scoops, instead of the expected straight channel. The suspected cause for this is that the inner surface of the guide ring was not machined prior to polishing. The tubing used to make the ring appears to have been rolled and welded from a flat sheet of steel. Therefore, the interior surface is irregular, and the weld seam can be seen. In order to eliminate this problem, the guide ring was removed, the interior surface was machined smooth, and it was re-installed into the chamber. The tests to follow were done without the urethane liner, with the hopes that this would also contribute to a better sphericity. After polishing with SiC - 1000 for 45 min the sphericity improved from 5.36 μm to 4.47 μm. While this is an improvement, we are still far short of the target.

By noting the relatively large amount of sphericity, the decision was made to mope to a larger abrasive. A larger abrasive particle will have the ability to remove a larger asperity, and given the high sphericity, there are obviously some large asperities left on the balls. In addition, other researchers have noted that using a 5% abrasive concentration, as opposed to 10%, has given better results with respect to sphericity. Two tests were run with B_4C - 800 at a volume concentration of 5% to check out this possibility. Both tests did show an

improvement: from 4.47 μm to 3.59 μm for the first, and from 3.59 μm to 2.16 μm for the second.

This is now getting much closer to the needed sphericity, but still needs improvement. Since the sphericity has improved to 2.16 μm, the decision was made to change to a smaller abrasive, since the reduced sphericity implies reduced asperity size. Three tests were run with SiC -1000 at 5% concentration. The sphericity results following each test were: 1.75 μm, 1.69 μm, and 1.85 μm.

Up until now the sphericity has improved, but seems to have hit a minimum value, and due to the removal of the urethane liner, the guide ring is showing a large amount of wear. The next step was to make a new guide ring with a machined inner surface, and replace the urethane liner. Three more tests were made with 5% SiC -1000 and the replaced liner, and the sphericity results were: 1.52 μm, 1.83 μm, 1.81 μm. Again we saw no improvement below the 1.5 μm point.

Variance of the spindle speed was the next parameter changed. Tests were made with 5% SiC -1000 at 1000, 3000, and 4000 rpm (all previous tests were done at 2000 rpm). The results for each test were 2.03 μm, 1.68 μm, and 1.69 μm respectively. Again there was no significant change in the sphericity measurements.

Once again we decided to try an abrasive with a still smaller grit size. The next test used 5% SiC with a grain size of <1μm (corresponding to about an 8000 grit). Again there was no significant change in the sphericity.

Suspecting that the grinding load was too high, the next test was performed at 0.5 N/ball instead of the normal 1 N/ball. The <1 μm SiC was used for this experiment as well, and again there was no change in the sphericity measurements.

As a last resort, an new float was tried. The float used for all of the above tests has a 45° surface that the ball rides on. If a comparison is made to the concentric apparatus, you can see that the polishing shaft used there has a 30°

surface. In order to check, this a new float was made with a 30° surface, and a test was run with it. Again no significant change in the ball sphericity.

At this point in the investigation we have exhausted all possible parameters that could cause poor sphericity. This brings the chamber design into question. The shaft eccentricity was based upon calculations by Zhang et al. (1996), to be 1.6 times the ball radius, and the chamber designed accordingly. As a result, the 0.4" eccentricity is the maximum amount that is possible with this chamber. We can, however, reduce the amount of eccentricity with only a small modification to the chamber. The aluminum plug around the guide ring needs to be modified to allow the spindle to move back towards a concentric alignment.

After the plug we modified, a series of tests was designed in order to establish the effect of eccentricity on both MRR and sphericity. These started by reducing the amount of eccentricity to 0.3", at which two tests were run with 5% SiC - 1000 and 2000 rpm, after which the eccentricity was reduced to 0.2", and so on until the spindle was concentric with the guide ring. Measurements were taken of the sphericity and MRR after each test, and the results from each test were averaged and grouped according to eccentricity. The results were tabulated and plotted in Figures 5.6a and 5.6b.

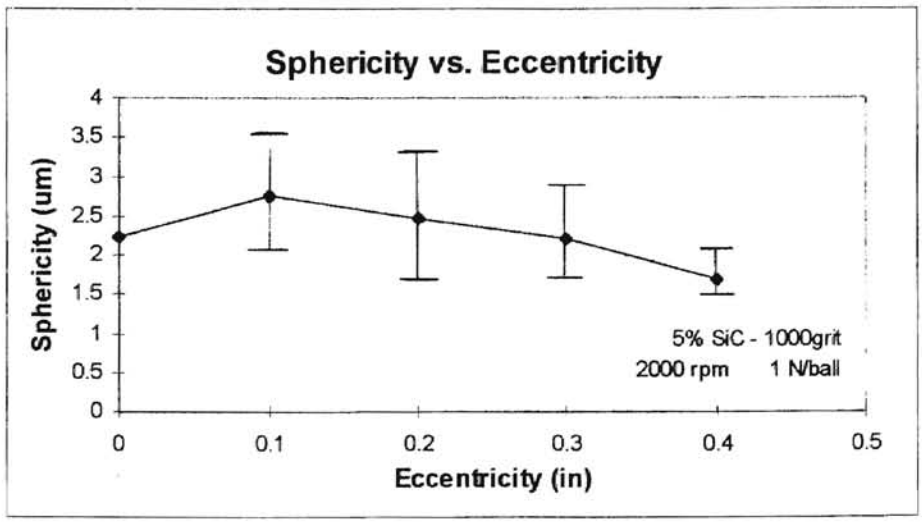

Figure 5.6a - Effect of Eccentricity on Sphericity

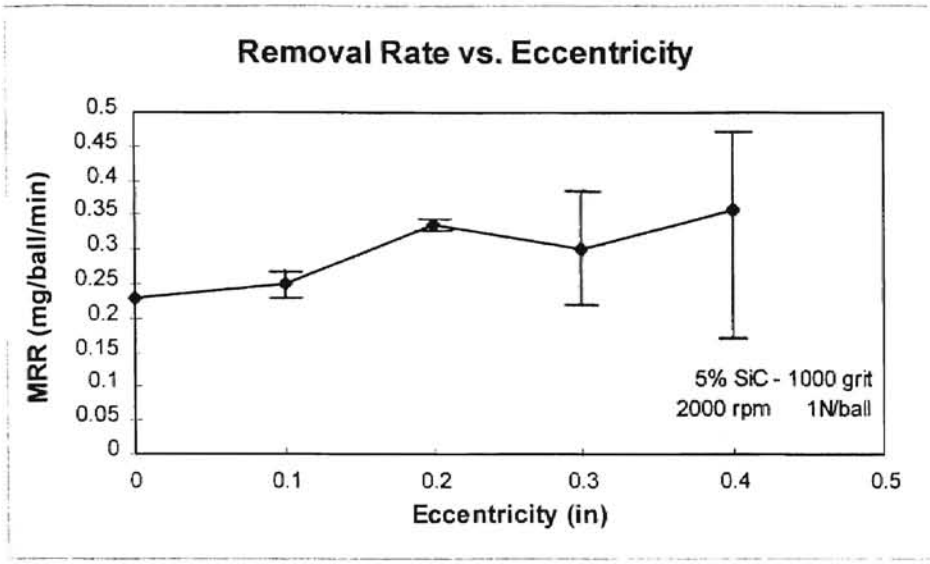

Figure 5.6b - Effect of Eccentricity on Material Removal Rate (MRR)

Note that in Figure 5.6a the sphericity reaches a maximum value at 0.1" eccentricity, and proceeds to reduce as the eccentricity increase. This corresponds roughly to the information published by Zhang et al. (1996). Given that each case uses chambers and balls of different sizes, the exact values at which the peaks occur are not identical, but the genera trend is quite similar. In addition, the effect of eccentricity on MRR also corresponds well with the results of Zhang et al. (1996), ncluded below in Figures 5.7a and 5.7b.

5.4 Discussion

Obviously the addition of the eccentric shaft as tested did not help the sphericity of the balls when compared to the results obtained from the conventional MFP. The most conspicuous of parameters to look at for an

answer to this dilemma is the eccentricity, as all other parameters are the same as in conventional MFP. A definite trend is seen in the curve generated for sphericity vs. Eccentricity in Figure 5.6a. If this curve is extrapolated out beyond

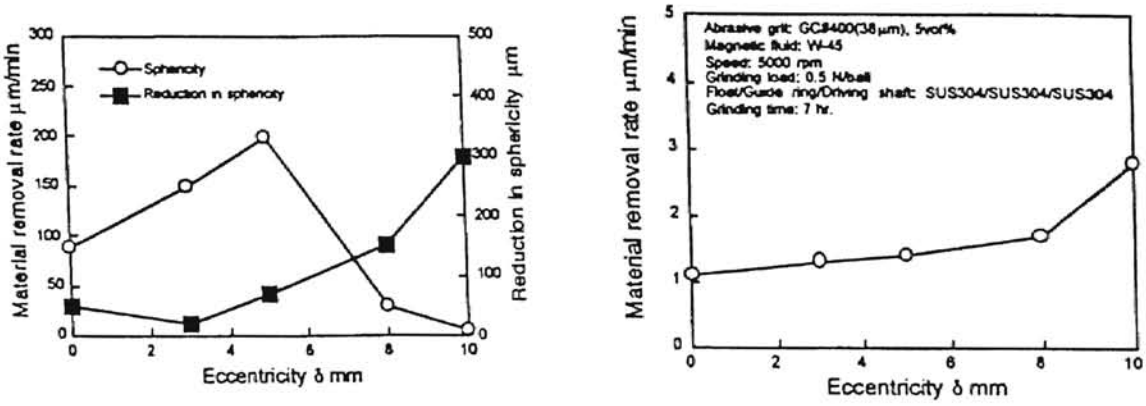

Figure 5.7 - a) Effect of Eccentricity on Sphericity b) Effect of Eccentricity on Material Removal Rate (Zhang et al. 1996)

the 0.4" mark, you can see that at an eccentricity just beyond the 0.7" mark, the sphericity should reach a value of about 0.5 μm. This would be acceptable and comparable results to the conventional MFP. If the eccentricity is set at 0.8", the sphericity will bet to a value of about 0.2 μm which is necessary for Grade 10 balls. Figure 5.8 below shows the same curve as in Figure 5.6a but extrapolated out beyond 0.4" eccentricity.

This initially seems to contradict the information quoted by Zhang et al. (1996) They based the amount of eccentricity on the radius of the balls. Specifically, the critical eccentricity, δ, is equal to 1.6 times the ball radius. The initial experiments run by Zhang et al. (1996) used a 10 mm diameter ball size. According to the critical eccentricity equation, the chamber should be set at 8

mm eccentricity. However, with this arrangement, they were able to get only 4.8 μm sphericity on the 10 mm diameter balls, and that occurred at an eccentricity of 10 mm as opposed to 8 mm. Similar to this investigation, their chamber was

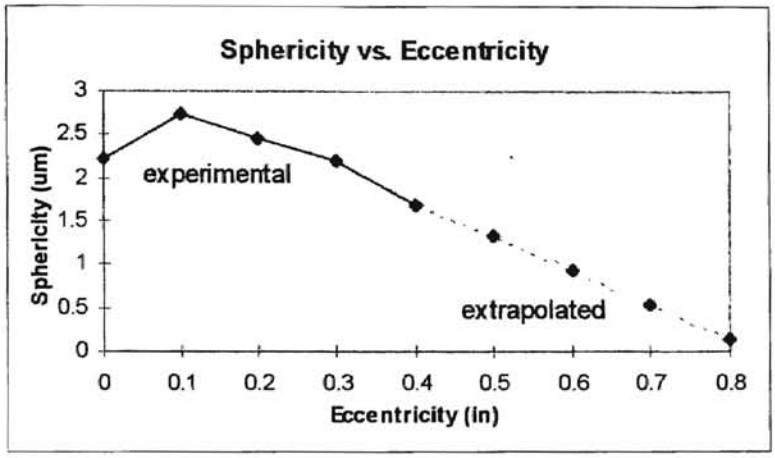

Figure 5.8 - Extrapolated Sphericity vs. Eccentricity Curve

only capable of a maximum eccentricity of 10 mm, so in order to investigate the eccentricity effect further, they changed ball size. Further experiments were done using a 6.5 mm ball diameter. Still the chamber eccentricity was set at 10 mm, and with this setup, they were able to get very good results - sphericity measurements of 0.12 μm. These results were obtained using a very fine (0.25 μm) diamond abrasive, and occurred after 42 hours of grinding time, with a starting ball sphericity of 5.7 μm.

If we assume that there is a direct relationship between ball size and eccentricity required for good results as proposed by Zhang et al. (1996), we can find the equation obtained from experimental results. At an eccentricity of 10

mm and a ball diameter of 6.5 mm the equation becomes: $\delta \approx 3R_b$. Experimental results gave a ball sphericity of 0.12 μm at these conditions. If this new relationship is applied to the case of 0.5" diameter balls, then the critical eccentricity is calculated to be 0.75". Applying this critical eccentricity to the extrapolated curve of Figure 5.8 we can get a ball sphericity of ~0.3 μm. The comparison between the two cases is quite strong and suggests that the critical eccentricity equation proposed by Zhang et al. (1996) needs some modification.

With regard to the MRR for the eccentric apparatus, it was found to be somewhat higher than the conventional MFP process, although not a vast improvement. Zhang et al. (1996) reported up to 4 times higher MRR over conventional MFP, however, the results presented here cannot justify such bold statements. These results show MRR to be higher for the eccentric chamber at lower spindle speeds, but at higher spindle speeds, the concentric chamber seems to have higher MRR.

Another set of 1/2" diameter balls was started on the eccentric chamber, but switched to the concentric chamber in order to get good sphericity, which has not been possible so far with the eccentric chamber. Several tests were run at both 2000 and 4000 rpm on both chambers and compared. All other parameters between the two were the same. Table 5.4 below gives a summary of the MRR for both chambers at different speeds.

If the data at 2000 rpm is evaluated, it appears that the MRR is about 2 times higher for the eccentric apparatus. But at the higher speed of 4000 rpm,

the MRR is higher for the concentric apparatus (although by a smaller margin). Due to this difference, there can be no absolute conclusions drawn as to the increase in MRR due to eccentricity.

Table 5.4 - MRR at Different Speeds for Conventional and Eccentric MFP

Spindle Speed rpm	MRR	
	Eccentric MFP mg/ball/min	Conventional MFP mg/ball/min
2000	1.097	0.672
4000	0.857	1.097

CHAPTER 6

ULTRASONIC ASSISTED MAGNETIC FLOAT POLISHING

In the spirit of continual advancement of the state of the art of MFP, the current investigation focuses on the addition of ultrasonic vibrations into the process. By introducing these vibrations we hope to improve the sphericity results achieved by MFP and possibly also increase the MRR. While the MRR is already very high (up to 40 times higher than conventional V-groove lapping) more improvement in this area would be acceptable, although not the prime goal of the modification.

6.1 Background Information

In order to understand how the MFP process may benefit from the addition of ultrasonic vibrations, it is necessary to get an overview of the many uses of ultrasonic vibrations, and how they are currently used in the industry today. The variety of applications is quite astounding, and the following sections only provide a quick glimpse at two main categories of ultrasonic applications. The first section deals with a situation where ultrasonic vibrations are used in machining applications, where material is being removed from a workpiece. The second section deals with other uses for ultrasonics.

6.1.1 Ultrasonic Material Removal

There are two categories of material removal processes that use ultrasonics. First is true ultrasonic machining, and the second is ultrasonic assisted machining. Ultrasonic machining uses the vibrations themselves as the material removal mechanism. In ultrasonic assisted machining, there is a primary means of material removal, such as a turning tool, to which ultrasonic vibrations are added to assist the process and improve characteristics. A key difference between the two is that ultrasonic assisted machining is still capable of removing material in the absence of the ultrasonic vibrations, where ultrasonic machining is not

6.1.1.1 Ultrasonic Machining Process

The process of ultrasonic machining uses the vibrations to excite an abrasive slurry in a confined area, usually with a shaped tool. The abrasive slurry then removes material in a mirror image of the shaped tool. This process is used extensively to create textured images in materials, such as nameplates, medallions, and other items. In this process the tool is not actually in contact with the workpiece, but with the abrasive slurry which is itself in contact with the workpiece. The typical frequencies used for this type of operation are between 20-40 kHz, which is above the range of human hearing, and thus the name ultrasonic. Figure 6.1 is a schematic of an ultrasonic machining apparatus.

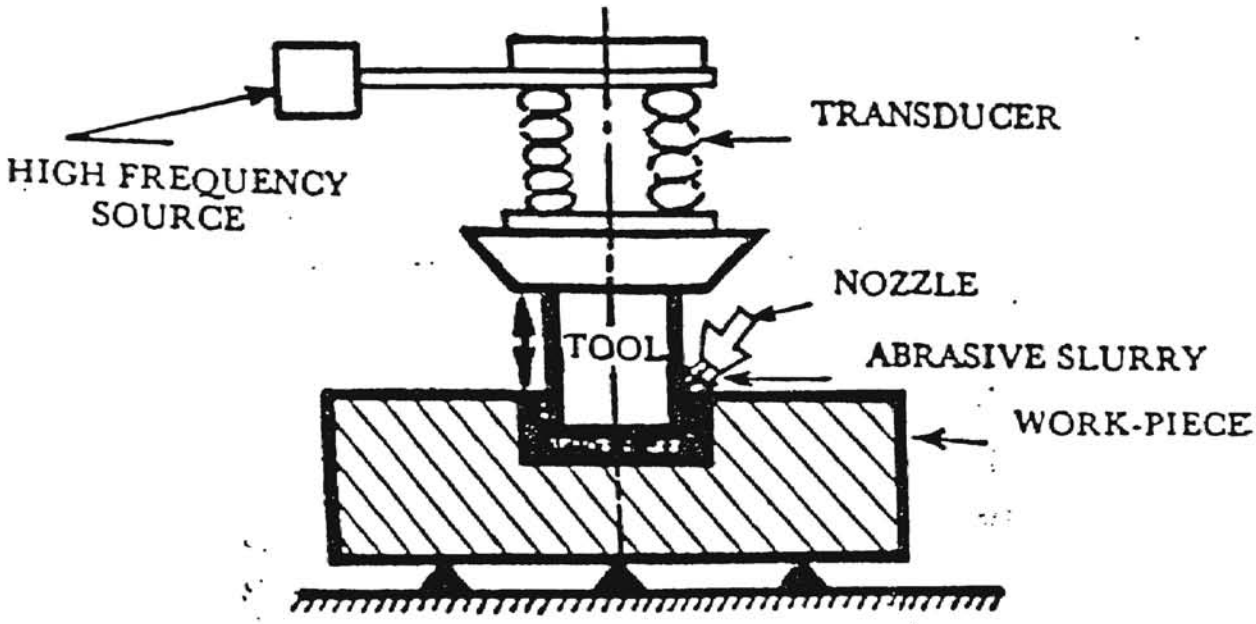

Figure 6.1 -Typical Ultrasonic Machining Apparatus

6.1.1.2 Ultrasonic Machining Components

The components required for ultrasonic machining include an AC electrical source, a frequency transformer which changes the 60 Hz AC current to the desired 20-30 kHz, a transducer to change the electrical oscillations to mechanical vibrations, a mechanical amplifier to magnify the amplitude of the vibrations, and a tool with a negative image of the desired shape. All of the above, combined with an abrasive slurry and mechanical feed system to advance to tool into the workpiece, make up a complete ultrasonic machining system. Typically the mechanical amplifier, or horn, is designed to achieve a

condition of resonance, which results in higher removal rates due to larger amplitude vibrations. A drawback to this is that, as the tool wears away, the vibration characteristics of the system change, and resonance can be lost. Therefore frequent "tuning" of the system is necessary in order to keep operating at the desired state.

Another feature often found on ultrasonic machines is a circulation system for the abrasive slurry. By keeping the slurry in motion, the wear debris can be removed from the machining area, and the slurry can be filtered and fresh abrasive added as needed.

6.1.1.3 Ultrasonic Assisted Machining

As mentioned above, ultrasonic assisted machining is a process that would still remove material if the ultrasonic vibrations were removed from the process. A typical application of this is ultrasonic assisted turning. In this situation the turning tool of a lathe is excited with small magnitude ultrasonic vibrations. By doing so, the cutting forces are reduced - resulting in longer tool life, and the chip removal characteristics are improved.

6.1.2 Ultrasonic Devices

Along with ultrasonic and ultrasonic assisted machining, there are a large number of devices that utilize ultrasonic frequencies to accomplish a variety of tasks. Among these are ultrasonic crack detectors, welders, and cleaners.

6.1.2.1 Crack Detectors

The crack detectors are used by material inspectors to find microscopic cracks and voids in materials. These devices typically consist of an ultrasonic transmitter and receiver pads. The two pads are placed on opposite sides of the material to be inspected, and the ultrasonic signal is sent. Signal strength varies through different materials, such as metals and air. As long as the receiver pad is getting a consistent signal, the material being tested is consistent and homogeneous. If the signal strength varies, this is an indication that there is a crack or void in the material to disrupt the nature of the signal transmission. A typical application for such devices is in the aircraft maintenance service, where microcracks will inevitably form, and could result in catastrophic failure if not detected.

6.1.2.2 Ultrasonic Welding

Plastics can be easily welded by utilizing ultrasonic vibrations. For example, if a cylindrical piece needs to be placed perpendicular to a flat plate, an ultrasonic welder will hold the cylinder, move into contact with the plate piece, and begin the ultrasonic vibrations. These vibrations when the two pieces are in contact creates friction, which melts the two parts at the joint, and creates a weld. Of course, this method will only work with thermoplastic materials, but the benefits are that the part is as strong as if it were formed in that shape in the first place, and no heat is needed - therefore there is little chance of deforming the

two pieces at any other place aside from the joint area. This method has also been used with good results on metal welding in certain applications, for example, welding a braided copper wire to a connecting terminal.

6.1.2.3 Ultrasonic Cleaners

Another widespread application of ultrasonic vibrations is in the use of bath cleaners. These cleaners come in any number of sizes to accommodate many different size parts. Parts are submerged in a tank that is filled with a cleaning solution. The tank is then excited with ultrasonic vibrations which perform the cleaning of the parts submerged within. The cleaning action occurs when small bubbles form in the fluid at the surface of the submerged part by cavitation, and subsequently collapse. This collapsing of the bubbles gives a small scrubbing effect to the surface of the part - thereby cleaning it. Solutions used range from as simple as distilled water to any number of chemicals including methanol or any combination of these. Tank sizes can range from a pint or less to several dozen gallons. The design of the tank is paramount in these cleaners. Figure 6.2 below shows a typical design of an ultrasonic cleaning tank.

Similar to the ultrasonic machining, resonance is a desired characteristic in order to get the greatest amount of displacement, therefore the tank that holds the cleansing solution is often suspended by the top rim of the tank, and the ultrasonic transducer is placed on the side or bottom of the tank. Being

suspended in this manner eliminates a good measure ef damping, and results in a more resonant system.

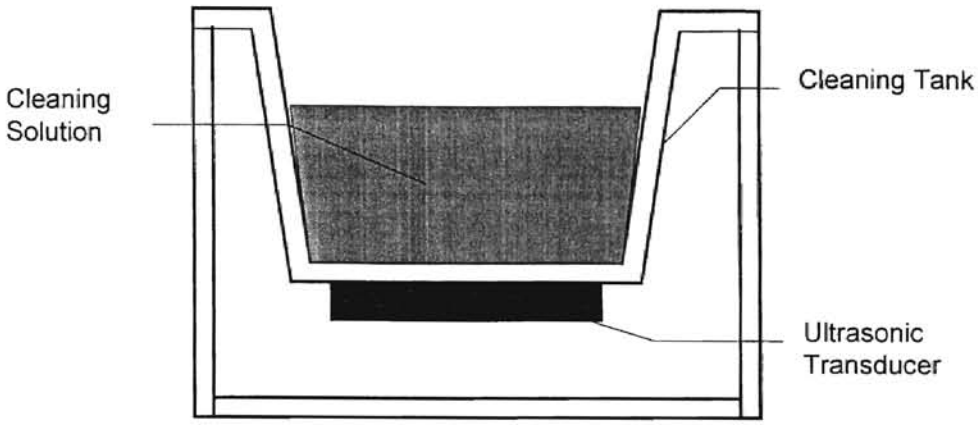

Figure 6.2 - Ultrasonic Cleaning Tank

6.2 Benefits of Ultrasonics in MFP

The benefits of adding the ultrasonics to the MFP process are expected to be twofold - increased MRR and decreased sphericity. First of all, the MRR may be increased for two different reasons. We hope to see a similar result as that seen in the ultrasonic machining process. The vibrations are expected to excite the float much in the same manner as a ultrasonic machining tool vibrates. When the float vibrates as such, we expect that it will cause impingement of the abrasive grains onto the surface of the ceramic balls. The second reason we expect that the MRR will increase is due to the principle of ultrasonic cleaning. The ultrasonics will cause the magnetic fluid to cavitate, forming a myriad of

small bubbles. When these bubbles collapse against the surface of the balls, they will cause abrasive grains to impact the surface of the ball as well.

This second material removal mechanism of abrasive grain impingement is added to the primary material removal mechanism of sliding contact. The ultrasonic vibrations should cause impingement by two different methods, and should not reduce the primary sliding contact - therefore we expect to see an increased MRR.

The second, and most important, area that we expect to see improvement in is the final sphericity of the balls. We expect that the scratch length produced by the sliding contact will be reduced, since the force will be oscillating. When this scratch length is reduced, the sphericity should see an improvement. Refer to Figure 6.3 for a graphical representation of scratch length.

a) b) c) d)

Figure 6.3 - Scratch Length Comparison

If, in each of the polygons shown above, the perimeter length stays constant, then the length of each side must be reduced as more sides are added to the polygon. This trend continues until there are an infinite number of sides, each with an infinitely short length, which results in a perfect circle. Now

applying this analogy to a three-dimensional sphere, and correlating the length of the sides to the length of the scratches produced by the polishing process, we can see that a reduction in scratch length should inherently produce a more perfect sphere.

6.3 Approach

One major choice to be made with the implementation of ultrasonic vibrations into the magnetic fluid polishing was where and how to apply the vibration. A key factor here is to provide minimal modifications to the current process. Since the process works fine as is, any changes may impair the products. This lead to the idea that the entire chamber should be excited, including the magnetic base and all. There are several reasons why this idea was abandoned. First of all, the chamber has a considerable amount of mass that would need to be moved. This would require a large and expensive transducer. Secondly, a transducer that large would require a large and powerful power supply. In addition, if the entire chamber is to be excited, the transducer will have to be mounted firmly to the mill table and be rigid enough to support the system. For these reasons an alternative was sought.

A much more viable method is to incorporate the ultrasonic transducer within the chamber just above the magnet base. The benefits to this situation are many. First of all, the transducer can be much smaller and less expensive, and require a smaller and less expensive power supply. Secondly, the transducer will be much closer to the work area, which makes for a greater

amount of the vibrations actually reaching the work area. Third, the transducer can be essentially part of the bottom of the chamber, which is very thin and made out of aluminum. This allows the bottom of the chamber to be somewhat flexible which means that not only will the transducer itself emit vibrations, but the entire bottom of the chamber will emanate vibrations - similar to the resonant state seen in the ultrasonic cleaning tanks.

6.4 Equipment Design and Construction

Two things to consider any time an ultrasonic transducer is to be used are the frequency and amplitude of vibration of the transducer. Ultrasonic machining is often performed at frequencies between 20 - 40 kHz. Ultrasonic cleaners usually operate in the range of 20 - 100 kHz. Since the application we intend to use the transducer for is similar to both of these situations, we looked for a transducer that operated in this range of frequencies. Amplitude of the vibration for this application is also going to be similar to that needed for the ultrasonic cleaner. Recall that, for ultrasonic machining, a horn is used to mechanically amplify the amplitude of the vibrations. But when implementing the ultrasonics into the MFP process, there will not be any room for an amplifying horn - indeed there is a very limited amount of space for the transducer itself. For this reason the amplitude and frequency of vibration needed for this application will need to be similar to those used in ultrasonic cleaning applications.

Inspection of several small ultrasonic cleaners revealed that the transducers used are actually very close to the necessary dimensions for

incorporation into the MFP process. In particular, one transducer was found that operated at a frequencq of 47 kHz, and was a circular disk with dimensions of 2" diameter, and 0.100" thickness. This is the transducer chosen to use in this investigation. An additional benefit of using this particular transducer is that a power supply from an ultrasonic cleaner can be used. These power supplies are abundant and relatively cheap from commercial suppliers.

The bottoms of the polishing chambers previously used all have a thickness of about 0.050". This allows the majority of the magnetic field produced by the permanent magnets to extend into the chamber. Adding a 0.100" thick transducer to this would result in a thickness of 0.150". This is of critical importance, due to the fact that the magnetic field produced is only about 0.250" itself. Having the bottom of the chamber this thick occupies the majority of the magnetic field, and moreover, occupies the strongest region of the field. If the stronger part of the magnetic field cannot be accessed, then the grinding load cannot be as large and MRR will suffer drastically.

In order to minimize this effect, the transducer was incorporated as part of the bottom of the chamber, instead of fixing it to the bottom as is. Figure 6.4 below shows how the transducer was placed. By placing it so, we can get higher compressive loads, and hopefully not suffer a reduced MRR. Epoxy was used to mount the transducer to the bottom of the chamber. This epoxy also serves to electrically isolate the transducer from the body of the chamber.

The two flat circular surfaces of the transducer are both coated with a conducting medium. When a voltage difference is applied across these two

(a) (b)

Figure 6.4 - Transducer Placement Options

surfaces, the transducer will respond with a geometrical change. With this particular transducer, the piezoelectric material is polarized to give a mechanical response in the axial (or thickness) direction. An additional benefit to placing the transducer as shown in Figure 6.4b is that both conducting surfaces of the transducer are exposed which make attachment of electrical wiring much easier.

This brings up the next topic to consider when designing this chamber, being how to get the ultrasonic signal to the transducer. Keeping the wiring as thin as possible is of great importance, so as not to consume more of the magnetic field. Conducting copper tape (similar to that used in Scanning Electron Microscopes) was used to accomplish this task. The tape is manufactured without any insulation, and had to be modified due to this fact, but this problem was solved by applying electrical tape to both sides of the conducting tape. The result is an insulated, and very thin, conductor that can easily be routed to both sides of the transducer with minimal effect on the physical characteristics of the chamber.

Now that these design aspects have been considered, the rest of the chamber had to be built according to ball size and number of balls per batch.

We chose to manufacture the chamber to polish 3/8" size balls, since that is the size used in other research simultaneously being conducted with the conventional apparatus. By doing this, all physical dimensions of this chamber were identical to the conventional chamber with the exception of the bottom of the chamber where the transducer was mounted. Similar machining techniques as covered in Chapter 4, for the manufacture of the concentric chamber were used for construction of this chamber as well, in order to ensure dimensional stability. As mentioned in Chapter 4 increased accuracy in the chamber itself gives better sphericity results. Figure 6.5 shows a diagram of the 3/8" chamber with the addition of the ultrasonic transducer.

One other modification was made to the process as a result of adding the transducer. Since the transducer takes up some of the magnetic field, but does not cover the entire bottom of the chamber, the float was modified to make maximum use of the magnetic field that is still left. Essentially, a pocket was machine out of the bottom of the float, allowing it to set down over the transducer, so that the float could get closer to the bottom of the chamber. The modified float is shown as part of the chamber in Figure 6.5.

6.5 Experiments Run

As of now, there have been very few polishing tests run with the ultrasonic assisted chamber, due to a variety of complications associated with the addition of the transducer.

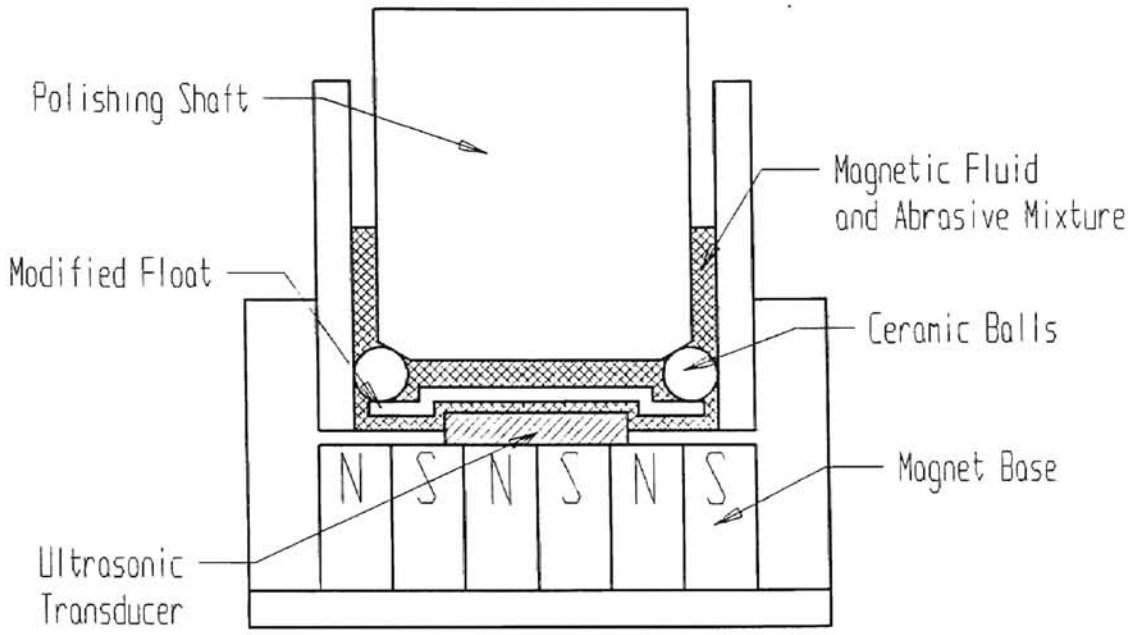

Figure 6.5 - MFP Chamber with Ultrasonic Modification

The first few tests revealed that the transducer was not mounted securely enough as part of the bottom of the chamber. During the test, the epoxy holding the transducer in place cracked, probably due to the pressure exerted by the mounting screws. This allowed the magnetic fluid to leak out of the chamber, and as a result very little polishing actually occurred.

To solve this problem, the transducer was remounted using a different method. Prior to applying the epoxy resin, the chamber was mounted to the magnet base, and the force sensing dynamometer, as it would be during a polishing test. All of the mounting screws were tightened, and the chamber was made secure. With the chamber in this state, the transducer was then re-

mounted, using a piece of wax paper to prevent the epoxy from contaminating the magnet base. This proved to be sufficient, as the transducer remained secure during subsequent tests.

There were however many problems associated with the power supply. During the polishing tests, several power supplies have burned out, and ceased to produce an ultrasonic signal. With no ultrasonic excitation of the transducer, it was pointless to continue testing the chamber. All efforts have been focused in the direction of repairing the power supply, and diagnosing why it failed. Once this has been revealed, steps can be taken to prevent it from happening again.

CHAPTER 7

CONCLUSIONS AND FUTURE RECOMMENDATIONS

Three different MFP chambers were investigated in the previous chapters. Each of these chambers has a new element associated with it that has previously not been investigated. While the current method of MFP is very good, there is always room for improvement, and that search for improvement is the motivation behind this investigation. While each of the chambers tested does show some promise, there is a need for further investigation with each of them. The following pages will summarize the results seen from each chamber, and give recommendations regarding future work with each of them.

7.1 Conventional MFP

A new chamber was built for use in conventional, or concentric, MFP. This chamber is no different in design than previous conventional chambers, with the exception that it was built to accommodate balls that are 3/8" in diameter, as opposed to 1/2" or 1/4". It is believed that there are many factors that can influence the ability of a chamber to produce good sphericity on the balls it polishes. With a more accurate and consistent chamber, the balls produced are expected to be of a higher quality.

Attention was focused intently on accuracy of the chamber during construction. Techniques were implemented so that all machining was carried out without removing the workpiece from the machine mount. By doing so, all surfaces were closer to being perfectly parallel, perpendicular, or concentric. This higher degree of accuracy will be reflected in the quality of balls produced.

After construction of the chamber was complete, testing ensued. The results of these test were initially very gratifying. Sphericity measurements during the initial rough grinding stages were approaching, and perhaps even exceeding, the best that we have been able to produce with this method of ball finishing. The best results seen thus far from this chamber have been an average of 0.47 μm. Comparing this to the usual value of 0.6 - 0.7 μm achieved from other conventional chambers, it can be seen that this new chamber holds good potential.

Sadly, the results did not remain as good when the process was moved into the fine polishing and finishing stages, where smaller, softer abrasives were used. During this phase of the polishing, the sphericity was seen to increase and hold steady at around 1.1 - 1.3 μm. This contradicts all knowledge that has been gained about the MFP process. In all other cases, when the established procedure is followed, the sphericity tends to improve as the abrasive particles reduce in both size and hardness. For some unexplained reason this did not occur here.

Future work needs to be carried out to investigate this strange behavior. If the trend continues to happen with this chamber, that is, good sphericity in the roughing stages, and increasing sphericity as the process moves into the fine polishing stage, the possibility of eliminating the fine polishing stage needs to be researched. This would seem to be a daunting task, as the fine polishing stage normally helps reduce the sphericity, and increase the surface finish qualities of the balls simultaneously. The rough grinding stage produces a very poor surface finish, and it is possible that the difference between this surface finish and the desired surface finish would be too large, and require an intermediate step. This intermediate step has shown in these tests to have a negative effect on the sphericity. Therefore, either a balance needs to be struck between sphericity and surface finish, or the problem of increasing sphericity needs to be ferreted out and eliminated. Obviously the later is the preferred alternative.

7.2 Eccentric Shaft MFP

The second topic covered in this investigation focused on offsetting the drive spindle, so that its axis rotates eccentric to the axis of ball rotation. The use of an eccentric drive spindle is sometimes used in the current industrial method of diamond lapping. Zhang et al. (1996) have adapted the eccentric shaft concept for use with MFP, and have reported increased MRR and much improved sphericity.

The principle behind the eccentric shaft is to increase the amount of sliding contact between the shaft and the balls, since this is known to be the

material removal mechanism (Childs et al., 1995). Also, the eccentricity helps to rotate the contact trace of the balls. The contact trace maps out how the point of contact between the ball and the shaft rotates around the ball (Zhang and Uematsu, 1996). By rotating this contact trace so that it encompassed the entire surface of the ball, it is thought that the sphericity will improve, due to a more uniform distribution of the material removal. Calculations were performed by Zhang and Uematsu (1996) to predict the amount of eccentricity needed for optimal finishing of balls. The critical eccentricity was predicted to be 1.6 times the radius of the ball.

Using the above infor-ation from these other researchers, an eccentric shaft MFP apparatus was constructed and tested. This chamber was designed to polish 1/2" balls, with an eccentricity of 0.4" - according to Zhang and Uematsu's formula.

The results seen from the eccentric chamber built did not live up to the expectations of better sphericity and improved MRR. While the MRR appeared to be higher at certain spindle speeds and lower at other spindle speeds, the sphericity was, without a doubt, not improved. The lowest value of sphericity achieved with this chamber was about 1.5 μm, compared to a minimum value of about 0.4-0.5 μm for the concentric chamber. This large difference is significant, and needs to be investigated further.

In the paper published by Zhang et al. (1996), they used a chamber designed to accommodate 10 mm diameter balls. According to the equation for

optimum eccentricity, they set the chamber for an eccentricity of 8 mm. Sphericity results were not satisfactory, so they increased the eccentricity to 10 mm, which happened to be the maximum the chamber was designed for. At this amount of eccentricity, the best sphericity obtained was 4.8 μm, which is far from the desired condition.

Since the chamber was operating at the maximum eccentricity, Zhang et al. (1996) decided to use a smaller diameter ball, which would effectively increase the eccentricity to ball diameter ratio. Using these smaller balls, they were able to get very good sphericity results - 0.12 μm. It should be noted however, that very fine diamond abrasives were used in this stage, and a total polishing time of 42 hours elapsed. During this 42 hours, the sphericity was reduced from 5.7 μm to 0.12 μm.

Analysis of the arrangement reveals that the eccentricity used to get these results was ~3(R_b), where R_b is the ball radius. This does not agree with the initial assumption that optimum eccentricity is ~1.6(R_b). However, excellent results were seen at the modified eccentricity.

Tests were run at different eccentricities with the chamber built for this investigation, and sphericity and MRR measurements were taken at each eccentricity. Plotting the sphericity values versus the eccentricity produces a chart that shows a definite trend. This graph was presented in Chapter 5 in Figure 5.6a. Extrapolation of this curve shows that, at an eccentricity of ~0.75", should result in a sphericity of ~0.3 μm.In addition, 0.75" eccentricity falls in line

with the modified equation for the optimal eccentricity as proposed in this investigation, which is: $\delta \approx 3(R_b)$.

To verify that this sphericity vs. eccentricity curve will behave as expected, a new chamber capable of larger amounts of eccentricity needs to be built. Figure 7.1 shows a proposed design for a new chamber.

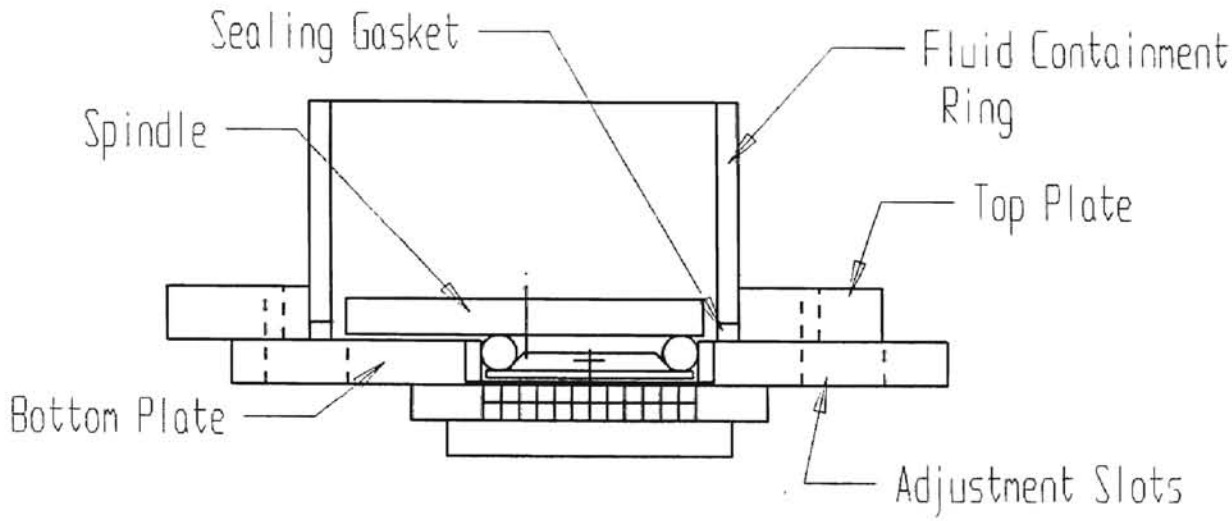

Figure 7.1 - Proposed Eccentric Shaft MFP Chamber

Two problems occur when the eccentricity of the chamber is increased. First of all, a larger eccentricity requires a larger spindle. When a larger spindle is manufactured, it is more difficult to keep it balanced. Small differences in weight can lead to significant vibrations when spinning at speeds up to 5000 rpm, and this problem is magnified when the spindle diameter is increased.

Unfortunately, there is no easy solution to this problem. A larger eccentricity requires a larger spindle. This could lead to more expense in the manufacturing stage, to acquire a spindle that is precision ground to high tolerances to help minimize this problem.

The second problem encountered with using a larger eccentricity is the fact that it requires using more fluid to submerge the balls, and since the magnetic fluid is the most expensive aspect of the MFP process, any minimization of use of magnetic fluid will result in a cheaper cost to finish the balls. The chamber outlined in Figure 7.1 attempts to minimize the use of magnetic fluid using a dual plate design. The top plate holds the fluid containing ring, and the bottom plate holds the guide ring, where the balls rotate. Altering the amount of eccentricity is accomplished by sliding the two plates across each other, and securing them with screws. By doing this, the fluid containment ring moves eccentric with the spindle, and can therefore be manufactured with a diameter just larger than the spindle diameter. If the chamber is built in this manner, excessive use of magnetic fluid an be avoided.

Difficulty may arise with the magnetic fluid leaking out between the plates. Great care needs to be taken when selecting and installing the gasket which lies just under the fluid containment ring, sealing it to the lower plate. This gasket is critical to the successful operation of this chamber.

This chamber should be able to verify the extrapolation of the sphericity versus eccentricity curve generated in Chapter 5. If it proves to be accurate,

then the eccentric chamber could be the next significant step in the evolution of the MFP process.

7.3 - Ultrasonic Assisted MFP

In Chapter 6 the use of ultrasonic vibrations and their use in many manufacturing applications was reported. Use of these ultrasonics leads to the idea that ultrasonics can be incorporated into the MFP process. Different methods of adding the ultrasonic transducer were considered, and a decision was made to install the transducer such that in becomes part of the bottom of the chamber. By selecting a sufficiently thin transducer, and mounting is as described, we can minimize the effect on the magnetic field.

Amplitude and frequency of the transducer were chosen to be similar to those seen in transducers used for ultrasonic cleaners. These transducers are designed to propagate ultrasonic vibrations through a liquid medium, similar to our situation. The transducer chosen was a piezoelectric ceramic crystal, of dimensions: 2" diameter, and 0.1" thickness.

A chamber was constructed for polishing 3/8" balls incorporating the ultrasonic transducer. Several tests were attempted, but the power supplies chosen for the job kept failing. This could be due to many reasons which have not yet been investigated. Future work consists of troubleshooting the power supply problems, and taking measures to avoid them in the future. Once this is complete, a full investigation of the ultrasonic assisted MFP can be carried out.

This includes evaluating the ultrasonic addition at all phases of polishing, with respect to MRR, sphericity, and surface finish.

If the addition of the ultrasonics proves to be valuable, other work may be carried out to find the optimal frequency and amplitude of vibration to use. This would require a variable transducer and/or power supply, which implies greater expense initially, but may prove to be fruitful.

REFERENCES

Baghavatula, R. S., "Chemo-Mechanical Polishing of Silicon Nitride with Chromium Oxide Abrasive," M.S. Thesis, Oklahoma State University, 1995.

Cetin, M., "Electromagnetic Field Assisted Polishing (EMFP) of Advanced Ceramics" , M.S. Thesis, Oklahoma State University, 1997.

Childs, T.H.C., Mahmood, S., and H.J. Yoon, " Magnetic Fluid Grinding of Ceramic Balls," Tribology International, 28, 1995, 341-348.

Childs, T.H.C., Jones, D.A., Mahmood, S., Kato, K., Zhang, B., and N. Umehara, "Magnetic Fluid Grinding Mechanics," Wear, 175, 1994, 189-198.

Dock, M., "Electromagnetic Float Polishing of Ceramic Ball Bearings," M.S. Thesis, Oklahoma State University, 1995.

Imanaka, O., Korube, Y., and K. Matsushima, "Magnetic Field-Assisted Fine Finishing," Proc. Of JSPE, Spring Conf. (in Japanese), 1981, 774-777.

Kato, K., Umehara, N., Adachi, S., and S. Sato, "Method for Grinding Using a Magnetic Fluid and an Apparatus Thereof," U.S. patent 4821466, Apr. 18, 1989.

Komanduri, R., Umehara, N, and R. Raghunandan, "On the Possiblity of Chemo-Mechanical Action in Magnetic Float Polishing of Silicon Nitride," Transactions of the ASME, Journal of Tribology, 118, 1996, 721-727.

Mitra, R., "Effect of Diameter-to-Thickness Ratio of Crystal Disks on the Vibrational Characteristics of Ultrasonic Ceramic Transducers," Applied Acoustics, 48, 1996, 1-13.

Raghunandan, M., "Magnetic Float Polishing of Silicon Nitride Balls," Ph.D. Dissertation, Oklahoma State University, 1996.

Stolarski, T.A., Jisheng, E., Gawne, D.T., and S. Panesar, "The Effect of Load and Abrasive Particle Size on the Material Removal Rate of Silcon Nitride Artefacts," Ceramics International, 21 1995 355-366.

Tani, Y., and K. Kawata, "Development of High-efficient Fine Finishing Process Using Magnetic Fluid," Annals of CIRP, 33/1, 1984, 217-220.

Umehara, N., "Research on Magnetic Fluid Polishing," Ph.D. Thesis (in Japanese, Tohuku University, 1990.

Umehara, N., "Magnetic Fluid Grinding - A New Technique for Finishing Advanced Ceramics," Annals of CIRP, 43/1, 1994, 185-188.

Umehara, N., Hayashi, T., and K. Kato, "In Situ Observation of the Behavior of Abrasives in Magnetic Fluid Grinding," Journal of Magnetism and Magnetic Materials, 149 1995, 181-184.

Umehara, N., and K. Kato, "Hydro-magnetic Grinding Properties of Magnetic Fluid Containing Grains at High Speeds," Journal of Magnetism and Magnetic Materials, 65, 1987, 397-400.

Umehara, N., and K. Kato, "Principles of Magnetic Fluid Grinding of Ceramic Balls," Applied Electromagnetics in Materials, 1, 1990, 37-43.

Umehara, N., and K. Kato, " Microsurface Finishing of Borosilicate Glass with Magnetic Fluid Grinding," Journal of Magnetism and Magnetic Materials, 122., 1993a, 432-436.

Umehara, N., and K. Kato, "Fundamental Properties of Magnetic Fluid Grinding with a Floating Polisher," Journal of Magnetism and Magnetic Materials, 122., 1993b, 428-431.

Umehara, N., and K. Kato, "Magnetic Fluid Grinding of Advanced Ceramic Balls," Wear, 200, 1996, 148-153.

Umehara, N., and R. Komanduri, "Magnetid Fluid Grinding of HIP-Si_3N_4 Rollers," Wear, 192, 1996, 85-93.

Zhang, B., Kato, K., and N. Umehara, " Dynamic Mechanics of Magnetic Fluid Grinding Process of Ceramic Balls," technical paper, 1996.

Zhang, B., and Uematsu, T., "Contact Trace and Sphere Surface Generation Mechanism in Ball Lapping," Submitted to Transactions of the ASME, Journal of Engineering for Industry, 1996.

Zhang, B., Umehara N., and K. Kato, "Magnetic Fluid Grinding of Ceramic Balls by Off-Setting Drive Shaft and Guide Ring Centers," Submitted to Transactions of the ASME, Journal of Engineering for Industry, 1996.

Ziegler, G., Heinrich, J., and G. Wotting, "Review - Relationships Between Processing, Microstructural, and Properties of Dense and Reaction-Bonded Silicon Nitride," Journal of Materials Science, 22, 1987, 3041-3084.

APPENDIX A

DETAILS OF POLISHING EQUIPMENT

A variety of equipment is used in the performing of the polishing tests. In particular, two different machine tools are used to provide the compression force and the rotation of the spindle to create the polishing motion. A dynamometer is used to measure the amount of compression force supplied. This dynamometer is mounted to the table of the machine tool, and the polishing chamber is in turn mounted on top of it. These pieces of equipment will be described in more detail below.

A.1 - Bridgeport CNC Milling Machine

One of the machine tools used is a Bridgeport CNC (Computer Numeric Controlled) Milling Machine. This machine is used in the manufacturing, as well as the testing, of the polishing chambers. The computerized positioning capabilities allow for high precision positioning of the spindle shaft. Rotation speeds between 100 - 6000 are possible. The machine tool is designed to manufacture small batches of parts quickly and easily. Due to its versatile design, and quick tool change capabilities, there may be more vibrations with this machine tool than with the PI spindle.

A.2 - PI Air Bearing Spindle

The other machine tool used in the polishing of the ceramic balls is the PI Air Bearing Spindle manufactured by Professional Instruments, Inc. As the name implies, the shaft rotates with very high precision air bearings. As a result, the rotation of the spindle is very accurate, and has little or no vibration. Speed capabilities of the spindle range from 0 - 20,000 rpm. This PI spindle is mounted on the body of an ordinary mill, which has an X-Y table for positioning of the chamber beneath the spindle. A drawback to this spindle, over the Bridgeport, is the manual positioning required to place the chamber.

A.3 - Kistler Dynamometer

To measure the compression force applied to the balls during polishing, a dynamometer is placed beneath the chamber. This dynamometer is manufactured by Kistler (type 9271 A), and measures compression and tension forces. Range of measurement is 20 kN for compression and 5 kN in tension, with a resolution of 0.02 N. The piezoelectric transducer sends a small electric signal to a Kistler charge amplifier (type 5004), which boosts the signal to a range that can be reported by a simple digital multimeter. Monitoring the readout on the multimeter gives the operator an easy means of setting the compression force.

APPENDIX B

DETAILS OF CHARACTERIZATION EQUIPMENT

Several pieces of equipment are used, both before and after polishing, to characterize the condition of the balls. The items measured include: weight, diameter, sphericity, and surface finish. The equipment used for each of these measurements will be described in detail below.

B.1 - Weight Measurement

Ball weight is measure before and after each polishing test. The difference between the two values, divided by the number of balls in the batch, and the polishing time leads to the MRR values. A precision balance manufactured by Brinkmann Instruments Company (Model 1712 MP8) was used for these measurements. This balance has a measuring range up to 160 grams, and a resolution of 0.1 mg.

B.2 - Ball Diameter Measurements

Ball diameter is measured using a digital micrometer manufactured by Mityutoyo (Series 293). Range of measurement is up to 25 mm, and the resolution of the instrument is 0.001 mm, or 1 μm. Measuring force is applied by

rotation of a thimble style constant pressure device. The measuring faces are carbide tipped steel with a flatness of 0.3 μm, and the parallelism between the two faces is 1 μm.

B.3 - Sphericity Measurements

Sphericity is defined as the difference between the radius at the point of maximum diameter of a shape, and the radius at the point of minimum diameter of a shape. The instrument used to measure the sphericity in this investigation was a Talyrond 250, manufactured by Rank Taylor Hobson Inc. The instrument is a stylus based machine, that uses a rotating chuck to hold and spin the part, while the stylus is in contact with the part. A linear transducer measures the position of the stylus as the part rotates. The stylus is mounted on a motorized column, which is used for positioning of the stylus. The whole system is controlled by a PC, which collects and analyzes the data, and generates the sphericity plots. Figure B.1 shows a schematic of the Talyrond 250. Not only is the machine capable of measuring sphericity, but vertical straightness, squareness, parallelism, flatness, co-axiality, cylindricity, and concentricity as well.

The rotating chuck has an axial error of 0.1 μm, and a roundness error of 0.04 μm + 0.0003 μm/mm height above the chuck. The system can collect a total of 2000 points per revolution, resulting in an angular resolution of 0.18^{o}. The stylus is 100 mm in length and has a sapphire spherical tip with a diameter

of 2.0 mm. The angular fluctuations of the stylus are monitored by a side acting transducer, that can operate in either high or low resolution modes. The low resolution mode has a range of measurement of ± 1 mm and a resolution of 0.6 μm. In high resolution mode, the range is reduced to ± 0.2 mm, and the resolution increases to 0.012 μm.

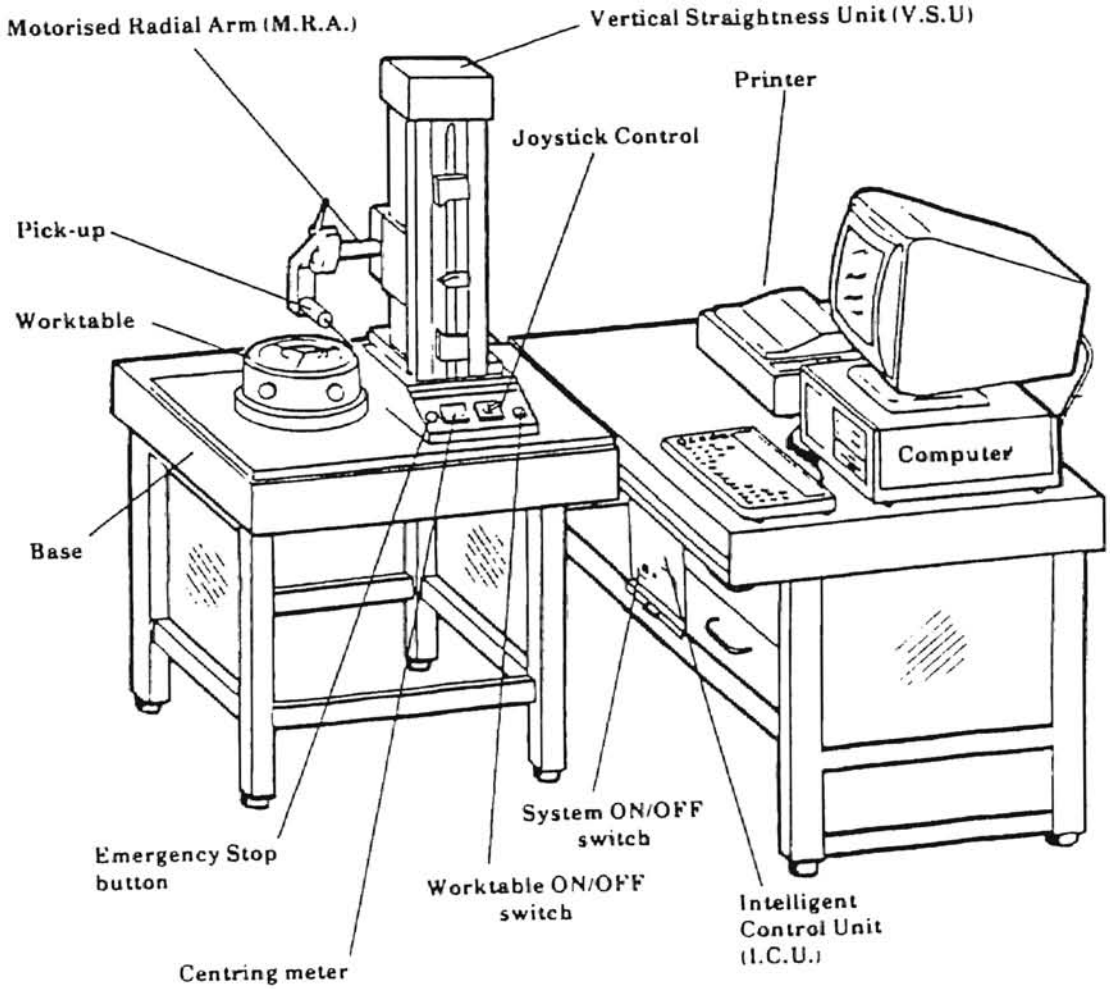

Figure B.1 - Schematic of Talyrond 250 by Rank Taylor Hobson

B.4 - Surface Finish Measurements

Another instrument manufactured by Rank Taylor Hobson was used to measure the surface finish of the balls. This machine is a Talysurf 120 L. It also uses a stylus based measuring technique. The overall design and layout of the machine are very similar to that of the Talyrond. A motorized column is used to position the stylus and move it over the workpiece. A PC is used to control the entire system, and to collect and analyze the data. One main difference is that the Talysurf uses laser interference to characterize surface form instead of a transducer as seen in the Talyrond.

A diamond tipped stylus is used with a tip radius of 1.5 - 2.5 μm. Vertical resolution of the stylus is 10.0 nm, and horizontal resolution is 0.25 μm. Range of measurement is 120 mm horizontal.

A variety of filters and data compensations are available for processing the data. Among these are included the ability to select the waviness filters, and form shape, cutoff length, wavelength and sample length. Figure B.2 show a schematic of the Talysurf machine.

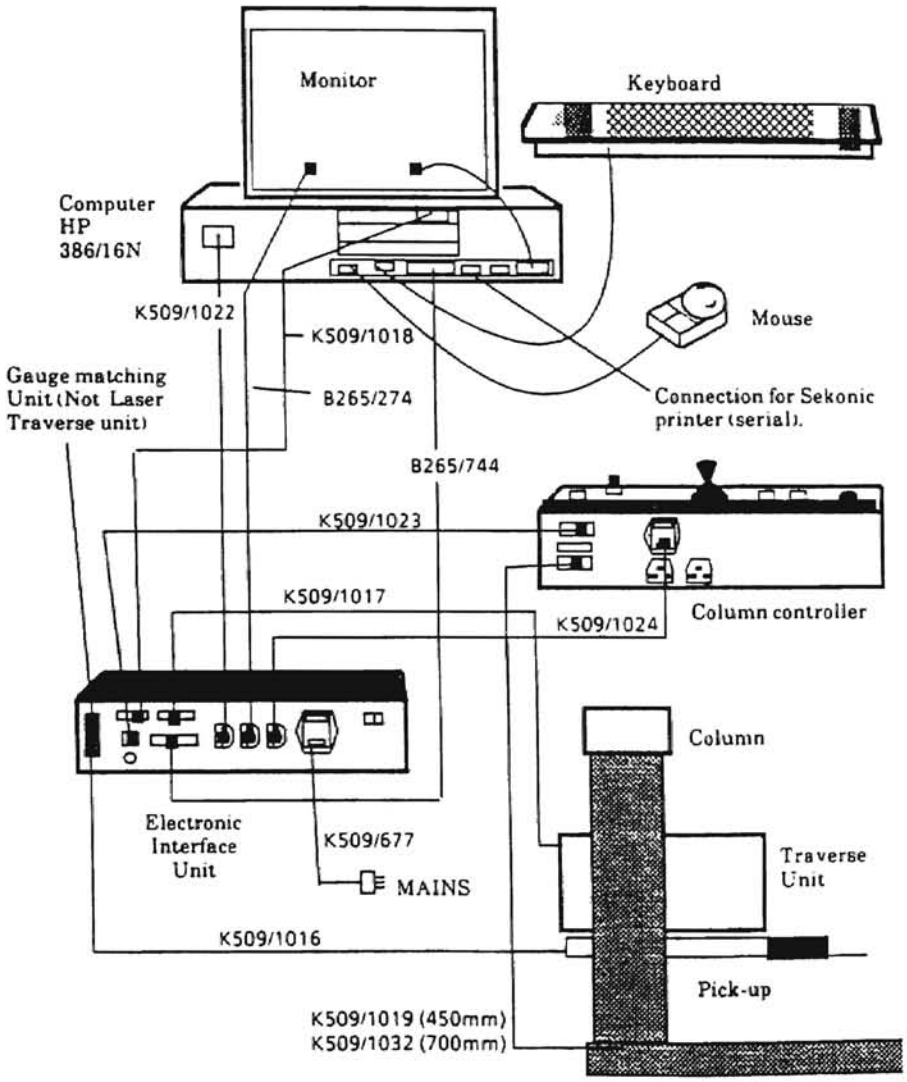

Figure B.2 - Schematic of Talysurf 120 L by Rank Taylor Hobson

VITA

Brian Perry

Candidate for the Degree of

Master of Science

Thesis: AN INVESTIGATION OF MAGNETIC FLOAT POLISHING TECHNIQUES INCLUDING CONVENTIONAL, ECCENTRIC SHAFT, AND ULTRASONIC ASSISTED POLISHING

Biographical:

Personal Data: Born in Muskogee, Oklahoma, on April 17, 1972, the son of Bobby and Mary Perry.

Education: Graduated from Chickasha High School, Chickasha, Oklahoma in May 1990, received Bachelor of Science degree in Mechanical Engineering from Oklahoma State University, Stillwater, Oklahoma in December 1995. Completed the requirements for the Master of Science degree in Mechanical Engineering at Oklahoma State University in December 1997.

Experience: Worked as Technical Service Representative at Mercruiser, Stillwater, Oklahoma during summers of 1991 and 1992; worked as an Co-op Engineer for Delta Faucet Company during summers of 1993 and 1994; worked as research assistant at Oklahoma State University from 1995 to 1997.